



저작자표시-비영리-변경금지 2.0 대한민국

이용자는 아래의 조건을 따르는 경우에 한하여 자유롭게

- 이 저작물을 복제, 배포, 전송, 전시, 공연 및 방송할 수 있습니다.

다음과 같은 조건을 따라야 합니다:



저작자표시. 귀하는 원저작자를 표시하여야 합니다.



비영리. 귀하는 이 저작물을 영리 목적으로 이용할 수 없습니다.



변경금지. 귀하는 이 저작물을 개작, 변형 또는 가공할 수 없습니다.

- 귀하는, 이 저작물의 재이용이나 배포의 경우, 이 저작물에 적용된 이용허락조건을 명확하게 나타내어야 합니다.
- 저작권자로부터 별도의 허가를 받으면 이러한 조건들은 적용되지 않습니다.

저작권법에 따른 이용자의 권리는 위의 내용에 의하여 영향을 받지 않습니다.

이것은 [이용허락규약\(Legal Code\)](#)을 이해하기 쉽게 요약한 것입니다.

[Disclaimer](#)

Electrochemical Sensors
for Flow-Enhanced Immunoassays
and Flow Monitoring of Porous Materials

Ja-Ryoung Han

Department of Chemical Engineering

Graduate School of UNIST

2014

Electrochemical Sensors
for Flow-Enhanced Immunoassays
and Flow Monitoring of Porous Materials

Ja-Ryoung Han

Department of Chemical Engineering

Graduate School of UNIST

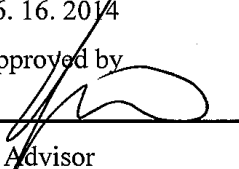
Electrochemical Sensors
for Flow-Enhanced Immunoassays
and Flow Monitoring of Porous Materials

A thesis
submitted to the Graduate School of UNIST
in partial fulfillment of the
requirements for the degree of
Master of Science

Ja-Ryoung Han

06. 16. 2014

Approved by



Advisor

Yoon-Kyoung Cho

Electrochemical Sensors
for Flow-Enhanced Immunoassays
and Flow Monitoring of Porous Materials

Ja-Ryoung Han

This certifies that the thesis of Ja-Ryoung Han is approved.

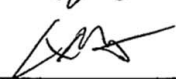
06. 16. 2014



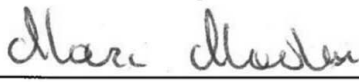
Thesis supervisor Yoon-Kyoung Cho



Yoon-Kyoung Cho



Chan Young Lee



Marc J. Madou

Abstract

Microfluidics enables a miniaturization of laboratory-scale biochemical analysis into a single chip. It has been actively developed and utilized in various biomedical diagnostic devices. Especially, lab-on-a-disc (LOD) and paper microfluidic system can serve as excellent candidates for point-of-care testing (POCT) because of several advantages including relatively simple fluid transfer mechanism, portable size of the device, fast analysis time, reduced cost, automated analysis steps and low consumption of test samples and reagents. In this thesis, electrochemical detection method has been implemented in two kinds of diagnostic devices. First, lab-on-a-disc integrated with screen-printed carbon electrodes (SPCEs) was developed for electrochemical detection of protein biomarkers, C-reactive protein. Compared to conventional optical detection, the electrochemical detection could provide enhanced sensitivity as well as significant cost reduction because it is not necessary to use optical grade plastic materials for the fabrication of the disc. In addition, we have developed electrochemical sensors for the measurement of the local fluid velocity based upon the fact that the electrochemical signal is proportional to the flow rate. As a proof of the concept experiment, we have used the electrochemical sensors for real time monitoring of the flow through porous materials, which can provide a practical tool to quantify the fluid velocity on the paper-based microfluidics. Based on chronoamperometric signals measurement using SPCEs, fluid transfer phenomena through various kinds of porous materials, geometries, absorption pads, and flow modifiers were evaluated. In conclusion, we have developed a cost-effective SPCEs-based electrochemical detection method and utilized not only for the immunoassays fully integrated on a disc but also to characterize fluid transfer behavior through the porous materials. The SPCEs can be utilized as a cost-effective sensor not only for the highly sensitive electrochemical detection for bioassays but also for the flow measurements in porous materials.

Contents

1	Introduction.....	14
1.1	Microfluidic Devices.....	14
1.1.1	Microfluidics for Point-of-Care Testing	14
1.1.2	Lab-on-a-Disc	15
1.1.3	Paper based Microfluidics	17
1.2	Immunoassays in Point-of-Care Testing	19
1.2.1	Enzyme Linked Immunosorbent Assays.....	19
1.2.2	Microfluidics based Immunoassay	21
1.3	Electrochemical Measurement.....	24
1.3.1	Chronoamperometry	24
1.3.2	ChronoamperometricDetection.....	25
1.3.3	Electrochemical Detection based Microfluidics System	26
1.4	Research Objective.....	28
2	Lab-on-a-Disc Integrated with Screen-Printed Carbon Electrodes for Electrochemical Detection of Protein Biomarkers.....	29
2.1	Introduction.....	29
2.2	Materials and Methods.....	35

2.2.1	Reagents.....	35
2.2.2	Fabrication of Screen-Printed Carbon Electrodes.....	35
2.2.3	Fabrication of lab-on-a-Disc.....	36
2.2.4	Measurement System.....	38
2.3	Results and Discussion.....	40
2.3.1	Electrodes Performance.....	40
2.3.2	Disc Operation.....	45
2.3.3	Diagnostic Performance.....	48
2.4	Conclusion.....	51
3	Electrochemical Velocimetry for Real Time Flow Measurement for Paper-Based Microfluidics.....	52
3.1	Introduction.....	52
3.2	Materials and Methods.....	57
3.2.1	Reagents & Materials.....	57
3.2.2	Device Fabrication.....	57
3.2.3	Measurement System.....	58
3.2.4	Electrochemical Velocimetry Converting Method.....	59
3.3	Results and Discussion.....	61

3.3.1	Flow Measurement	61
3.3.2	Characterization of Flow Rate	64
3.4	Conclusion.....	71
4	Concluding Remarks	72
	References.....	73
	Acknowledgements.....	79
	Curriculum Vitae.....	80

List of Figures

Figure 1 Examples of commercialized POCT type diagnostic devices based on microfluidic system	14
Figure 2 Scheme of the centrifugal pumping of liquid on a rotating disc.....	16
Figure 3 Schematic illustrations of capillary absorption in a porous material strip.....	18
Figure 4 Schematic diagrams of various ELISA types characterized by the reaction order of antigen or antibody.	20
Figure 5 Examples of microfluidics based immunoassay	23
Figure 6 Schematic diagrams of electrochemical measured chronoamperometric signal.	25
Figure 7 Electrochemical detection on microfluidic system.....	27
Figure 8 Simultaneous multiple operation lab-on a disc based immunoassay.....	32
Figure 9 Examples of fully automated ELISA on disc	33
Figure 10 Examples of electrochemical sensor integrated lab-on-a-disc devices.....	34
Figure 11 Fabrication of screen printed carbon electrodes (SPCEs).....	36
Figure 12 Schematic design of lab-on-a-disc for electrochemical detection integrated with SPCEs and the exploded illustration of the disc.....	37
Figure 13 Electrochemical measurement system for the rotating lab-on-a-disc.....	39
Figure 14 SEM photographs of the surface of a carbon electrode.....	42

Figure 15 Reference electrode addition results with cyclic voltammograms..	43
Figure 16 Electrode performances of lab-made SPCEs and commercially ordered product SPCEs...	44
Figure 17 Detailed illustration of SPCEs integrated microfluidic disc with valves.....	46
Figure 18 Operation of centrifugal microfluidic disc with color dyed water.....	47
Figure 19 On-disc electrochemical immunoassay's calibration curved obtained by different detection methods.....	50
Figure 20 Paper or porous material based commercially available diagnostic lateral flow strip sensors.	54
Figure 21 Applications of paper microfluidic system besides diagnostic test kit.	55
Figure 22 Current techniques to measure paper fluidics flow rate based on optical detection.....	56
Figure 23 Schematic illustration of device	58
Figure 24 Schematic illustrations of flow operation, induced by a paper sample in the device system	60
Figure 25 Electrochemically measured fluid flow induced by porous materials.....	62
Figure 26 Calibration curves of electrochemically measured results using the proposed device.....	63
Figure 27 Analysis of geometric effect in flow rate.....	66
Figure 28 Analysis of additional absorbing pad's effect.....	67
Figure 29 Analysis of flow mechanisms from different paper products	68
Figure 30 Characterization of fluid modification by applying oxygen plasma treated, 16% w/v dextran	

coated, and normal nitrocellulose membrane. 69

Figure 31 Characterization of fluid modifiers by using electrochemical measurement system. 70

List of Tables

Table 1 Summary of the results from the evaluation of screen-printing carbon paste onto various substrates: definition of printing and penetration into material.....	42
Table 2 Operation programs of lab-a-disc device for fully automated immunoassay with electrochemical detection.....	46
Table 3 Results of ELISA by electrochemical detection with different detection methods.....	49

1 Introduction

1.1 Microfluidic Devices

1.1.1 Microfluidics for Point-of-Care Testing

Microfluidics enables a miniaturization of laboratory-scale analysis technologies onto a small sized device.^{32,33} Also known as lab-on-a-chip (LOC), the system can integrate several laboratory tests into a single chip.^{14,36} Recently, there are increased number microfluidics devices that utilize microfluidics technologies in various platforms such as lab-on-a-disc and lateral flow strip sensors, which can be categorized depending on pumping system.^{37,38,39} Lab-on-a-disc is a branch of LOC which is unique in a sense that it uses centrifugal force to propel liquids.⁴¹ Paper based lateral flow strip sensor is one of the commonly used platforms for point-of-care testing (POCT) devices due to the capillary pumping force derived by porous structure, which makes liquid propulsion without external pumping hardware.⁴²

These days, there are a number of commercialized POCT devices based on microfluidics system.⁴³ Lab-on-a-disc based POCT devices are actively under development.⁴¹ LabGeo IB10 from Samsung (Figure 1A, p.12) is the successful example of commercialized product of lab-on-a-disc based POCT diagnostic tool.⁴ Only by injecting whole blood sample, all the immune analysis processes are automatically run within 30 minutes. With high accuracy and fast analysis time, it evaluates the complicated analyzing process into automated POCT tool. Paper based lateral flow strip sensor is one of the most widely used microfluidics based POCT tool.⁴⁴ Pregnancy test kit is the representative

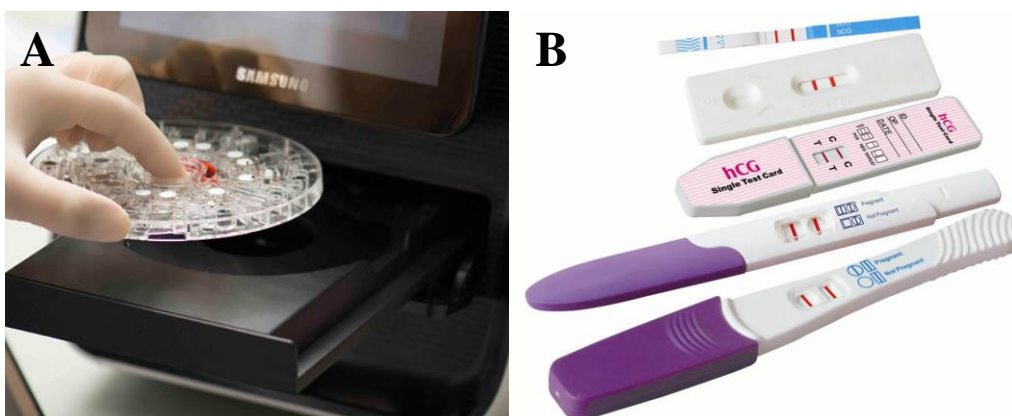


Figure 1. Examples of commercialized POCT type diagnostic devices based on microfluidic system. (A) LabGeo IB10 immune system testing lab-on-a-disc device and its analyzer.⁴ (B) Lateral flow strip sensor type pregnancy test kit.^{13,16}

example of lateral flow strip sensor as shown in **Figure 1B**.¹⁶ Once user loads urine sample to the test kit, liquid is absorbed by capillary force of porous membrane which is the composition of the strip sensor. The test zone will show a band type result by applying antigen-antibody immune reaction. It is the cost-effective, easy to use, and portable diagnostic device that could be used not only for common market but also for the third world countries.⁴⁴

As it can be seen from above examples, lab-on-a-disc and paper-based lateral flow strip sensor can serve as an excellent candidate for POCT because of several advantages including portable size of the device, fast analysis time, reduced cost, automated analysis steps and low consumption of samples. Detailed operation mechanisms of each system will be introduced in the next chapters.

1.1.2 Lab-on-a-Disc

Theory

“Lab-on-a-disc” requires a single motor to generate fluid propulsion in the system. Therefore, the total system can be more compact and simple.⁴¹ For lab-on-a-disc system, **centrifugal force** drives fluid dynamics, which is influenced by rotation speed, channel and reservoir’s location, geometry of the channels, and fluid properties. The average velocity of liquid in channels under centrifugal pumping system, U is given as (**Figure 2**)

$$U = \frac{D_h^2 \rho \omega^2 \bar{r} \Delta r}{32 \mu L} \quad (\text{Eq. 1})$$

where D_h is the hydraulic diameter of the channel, ρ is the density of the liquid, ω is the angular velocity, μ is the viscosity of solution, L is the length of the liquid in the channel, \bar{r} is the average distance of liquid in the channels ($\bar{r} = (r_1 + (r_0 - H))/2$), and Δr is the radial extent of the fluid ($\Delta r = r_1 - (r_0 - H)$). As show in equation (1), spin speed plays a critical role in the lab-on-a-disc operation.^{13, 14}

Unit operation

Strengths of Lab-on-a-disc system are the integration of valve, mixing, metering into the system much more easily than LOC system. To control the fluid transference on a rotating disc, various kinds of **valves** have been developed using capillary geometry, hydrophobic surface treatment, siphoning channel, and sacrificial materials.⁴¹ Capillary, hydrophobic, or siphoning valves are examples of passive valve, which does not require external energy source but only depends on the rotation speed of the disc. The required frequency can be calculated via force balance between the surface tension and the centrifugal force. The valve is closed-state when the disc spins at the frequencies lower than

the burst frequency.¹³ It is easy to control because the valve changes to an open state only by adjusting the spin speed. On the other hand, laser irradiated ferrowax microvalve (LIFM) is a representative example of active valves using sacrificial material. It is composed with magnetic nanoparticles and paraffin wax, which can control by laser light source.

In lab-on-a-disc system, there is a unique volume control function; **metering** put its basis on overflowing of fluid. After sample injection on the disc, rotating makes overflow of excessive portion of sample to the connected channel or chamber. Through this technique, it is possible to meter volume, which is essential operation for many kinds of diagnostic assay.^{17, 41} Another great characteristic of centrifugal microfluidics system is **mixing**. Although uniform mixing of reagents is important in many bio-analytical processes, it is difficult to mix several components in lab-on-a-chip system because of the laminar flow without convection.^{45, 46} However, an efficient mixing can be easily achieved in the disc via repeating rotation in clockwise and counter-clockwise direction.²⁵ Furthermore, addition of precursors such as magnetic particles in a mixing chamber improves effective mixing.^{25, 47} Overall, lab-on-a-disc is very useful for POCT system due to the simple operation, fluid storage capability, easy mixing and metering.

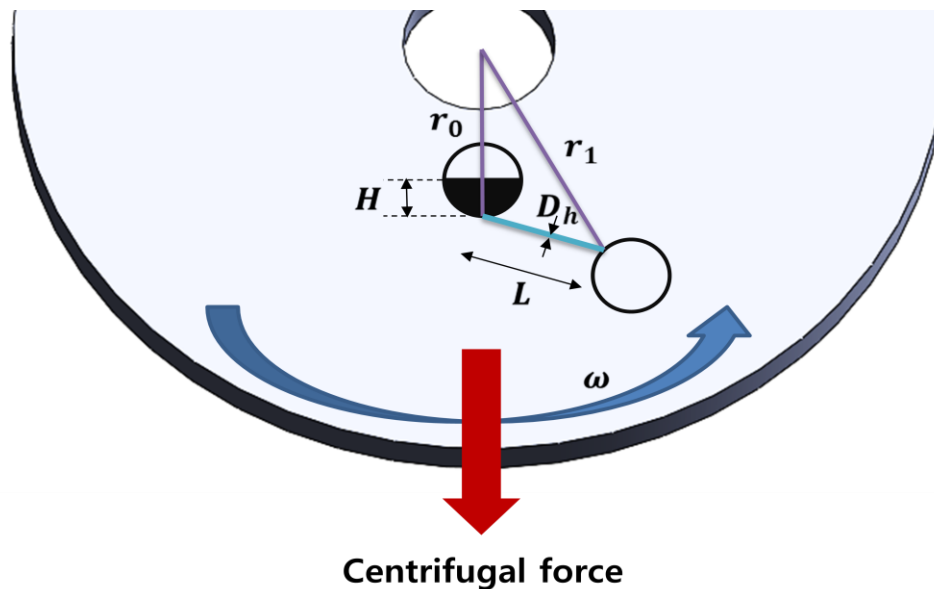


Figure 2. Scheme of the centrifugal pumping of liquid on a rotating disc. r_0 and r_1 are the inner and outer radii of the flowing fluid; H is the “head” of the liquid in the feed reservoir; D_h is the hydraulic diameter of the channel; L is the length of the channel; ω is the rate of rotation.^{13, 14}

1.1.3 Paper based Microfluidics

Paper microfluidics device is composed with porous materials such as paper. Typically, porous materials absorb liquid due to capillary force and it serves as a driving force in the paper based microfluidics system without the needs of external pumping hardware.⁴⁸ This system is usually applied to lateral flow strip sensor containing porous material such as cellulose. It is one of the most commonly used microfluidics based POCT device used in real medical diagnostic area.⁴⁹ It is often used for simple and quick diagnosis to figure out the existence of targeted bio-markers in the sample.^{44, 50, 51}

The capillary action means the fluid flow phenomena occurred inside the micro-channel or through the pores of porous material not because of interaction via external force but because of intermolecular force between surfaces of fluid and substrate.^{15, 52} In general, flow that exhibits capillary driven-flow, takes place in two phases: wet-out flow and fully-wetted flow (**Figure 3**).² Wet-out flow means that the flow begins front in the dried paper with the first contact to liquid immediately. In this part, flow goes faster than fully-wetted flow and it has inversely proportional speed to the strip length as shown in Washburn equation.⁵³ It is given as

$$L^2 = \frac{\gamma D t}{4\mu} \quad (\text{Eq. 2})$$

where, L is the distance moved by fluid front, t is time, D is the average pore diameter, γ is the effective surface tension, and μ is viscosity. When the paper has been wetted enough by the wet-out flow, fully wetted flow is generated by the capillary action with a downstream feature. It is governed by Darcy's law, given as

$$Q = -\frac{\kappa W H}{\mu L} \Delta P \quad (\text{Eq. 3})$$

where, Q is volumetric flow rate, κ is the permeability of paper, W is the width, H is the height, ΔP is the pressure difference along direction of flow, and L is the length. In the majority of cases, flow rate of paper materials has direct relation to detection sensitivity of strip sensor offering clearness of band and reproducible results from batch to batch.⁵⁴ To conclude, paper based microfluidics has capillary action as a driving force, which is very important factor as a POCT tool not only for pumping source but also for detection sensitivity.

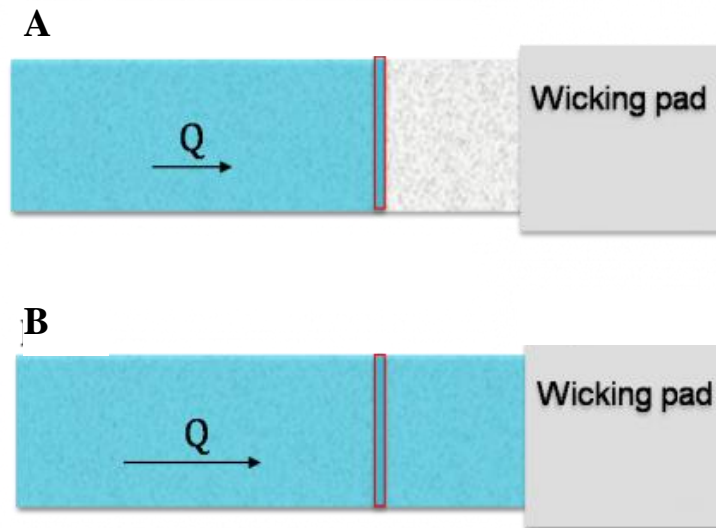


Figure 3. Schematic illustrations of capillary absorption in a porous material strip. ² (A) Wet-out flow state that begins with the first contact to liquid phase. (B) Fully wetted flow state followed after wet-out state flow, governing by Darcy's law.

1.2 Immunoassays in Point-of-Care Testing

1.2.1 Enzyme Linked Immunosorbent Assays

Immunoassay is a kind of biochemical testing technique to determine the concentration of target macromolecules such as protein in biological samples including blood serum via immune-reaction by utilizing target specific antibody. Antigen-antibody interaction is a reaction that uses a small amount of target species can generate stable signals. It is possible that quantitative and qualitative analysis by applying labelled antigen or labelled antibody. Immunoassay can be categorized according to the labelling method: radioactive label for radioimmunoassay (RIA), an enzyme label for enzyme immunoassay (EIA), and fluorescent label for fluorescence immunoassay (FIA).^{55, 56} Especially, enzyme-linked immunosorbent assay (ELISA), a type of EIA, has been widely used over four decades as a clinical analysis method because of its good specificity, sensitivity, high-throughput analysis capability, and wide range of target analytes.^{57, 58}

ELISA is categorized as direct, indirect and sandwich ELISA depending on the orders of antigen and antibody reaction. For direct ELISA detection (**Figure 4A**), the target antigen is coated onto the immobilization substrate such as polystyrene 96-well plate. After the coating, the target specific enzyme conjugated primary antibody is loaded to the target antigen coated onto substrate directly. It is a simple and fast analysis technique among ELISA techniques with the few process steps. However, it has relatively low sensitivity due to the minimized signal amplification. Besides, this technique has only a limited number of the usable primary antibody labels because it is required the specific responsiveness to the antigen and the enzyme at once.

For indirect ELISA detection (**Figure 4B**), the target specific primary antibody is loaded to the plate pre-coated with the target antigen. After the reaction between the target antigen and primary antibody, enzyme-conjugated secondary antibody is loaded to the plate. Then, secondary antibody is bound to primary antibody. It is advantageous in terms of the better sensitivity than direct ELISA. Options for the secondary antibody increase because it, which requires only the reactivity to the primary antibody. In addition, unlimited choices for primary antibody are possible, which require only the reaction with enzyme-conjugated secondary antibody. However, a critical drawback is the non-specific binding from cross reactivity of secondary antibody resulting with false positive signals.

The “sandwich-ELISA” or “two-site ELISA” assay (**Figure 4C**), which is a highly sensitive and efficient detection technique, needs the antigen containing at least two sites for antibodies. It is the most sensitive ELISA technique so far, overcoming non-specific binding through the primary

antibody on substrate to capture target antigen. To run the sandwich ELISA, the plate is coated with primary antibody (or capturing antibodies) that can capture target antigen as a preliminary step, and then antigen is loaded to the plate. Finally, enzyme-linked secondary antibodies are bound to antigens. Excess or unbound antigen and secondary antibody are washed away by rinsing with washing buffer. To evaluate the concentration of target species, label active substrate is loaded to the plate. It is the most widely used ELISA method for diagnosis due to its clinical significances with great sensitivity and specificity. It is very useful and famous bio-analytical technique; nevertheless long assay time and complicated handling processes are the shortcomings.

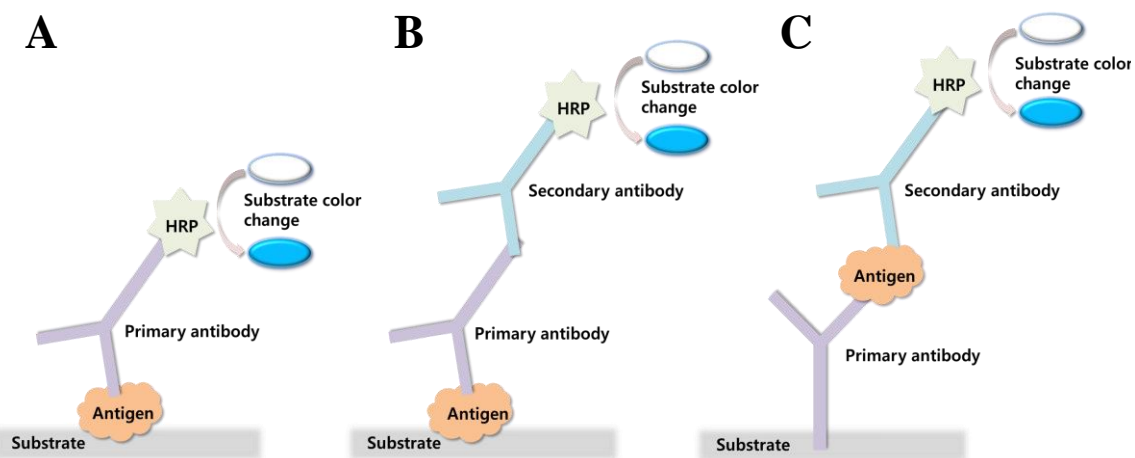


Figure 4. Schematic diagrams of various ELISA types characterized by the reaction order of antigen or antibody. (A) Direct ELISA, which makes the direct coating of target antigen onto substrate and direct reaction with HRP conjugated primary antibody. (B) Indirect ELISA, which has HRP conjugated secondary antibody to react with primary antibody. (C) Sandwich ELISA, which is composed with three reaction steps: primary antibody coating onto substrate, antigen reaction with primary antibody, and HRP conjugated secondary antibody bonding to antigen.

1.2.2 Microfluidics based Immunoassay

Microfluidics has continuously developed especially for medical diagnostic tools with a number of advantages. It has become popular and specialized, facilitating a broad range of quantifiable analytical technologies.^{36, 39, 43, 59} Despite such improvements, the ELISA, which has great advantages for clinical diagnosis is still suffering from some difficulties to integrate into the microfluidic system as POCT tool: complicated steps, time consuming procedures, proper detection technique for micro-scale system, and requirement of diverse fluid dynamics like mixing and metering. To overcome these problems, various studies are introduced.

Early studies about ELISA on **lab-on-a-chip** can be represented in terms of technical integration into micro-scale system with reduced reagent consumption and assay time. In 2000, for example, Sato *et al.* demonstrated the chip based immunoassay with polystyrene beads embedded microfluidic channel inside.⁶⁰ Respectable sensitivity for human secretory immunoglobulin A (s-IgA) could be offered in 1 hour, thereby using the micro-scale beads with high surface area compared to the size of beads. However, not only these studies^{61, 62, 63, 64, 65} but also these chip based studies had some inconveniences caused by additional handling for washing and mixing and it is a critical disadvantage as a POCT tool. So that, several studies were demonstrated to carry out the automated ELISA via sequential reagents transferring.⁴² Linder *et al.* demonstrated an automated immunoassay chip through negative pressure (**Figure 5A**).⁵ In this study, all reagents were sequentially displaced at the specific locations at channel inside, and then passive flow delivered the solution in the order of assay process. Gervais *et al.* introduced an one-step immunoassay microfluidic chip based on capillary force.⁶⁶ Herein, they used human serum sample containing detection antibody. With this chip, the LOD of C-reactive protein was 10ng/mL with fluorescent detection and total assay time was less than 3minutes. Though these developments achieved ELISA assay chip with sensitive, fast and affordably reduced reagents consumption, it is essentially required additional pumping machines, complicated tubing networks altogether inlets and outlets, and detection hardware resulting in the massive whole system.⁶⁷ Also, micro-scale size channel makes laminar flow propulsion, which has limitations for effective washing, mixing and reacting across the whole assay.⁴⁶ That is the reason why lab-on-a-chip based ELISA devices are hard to be established as POCT tools even it has been developed continuously.

Lab-on-a-disc technology offers fluid transferring and other dynamics control by simply applying centrifugation.⁴¹ Using centrifugal force, lab-on-a-disc takes easy operation and automation, becoming a good candidate for immunoassay POCT tool. Early examples of disc-based ELISA devices are focused on whole assay processes with a serial of controlled rotations by using geometric

structured valves such as siphon channel or capillary valve.^{8, 20} Lai *et al.*, demonstrated the immunoassay disc fabricated in PMMA (**Figure 5B**).²⁰ In this disc, there were passive valves to control fluid propulsion under sequentially increasing rotational speed. The diagnostic performance of Immunoglobulin G (IgG) from hybridoma was comparable to traditional 96-well plate-based assay results, while accepting less volume of solution and shorter operating time. Moreover, 24 sets of assay test units were integrated on a disc. This study showed good approaches of ELISA disc, which is operated by serial rotation. Lee *et al.* presented an advanced study. To detect Hepatitis B virus (HBV) from whole blood, the fully-automated immunoassay disc was invented for the first time. The only required manual handling is sample injection among whole assay steps (**Figure 5C**).²⁵ Based on this study, commercialized immunoassay POCT product from Samsung was introduced.⁴ It is a portable system that can be use easily without any additional sample pretreatment processes.

Paper-based microfluidics has recently garnered significant interest because the materials cost is low and it does not require expensive hardware to control fluid flows.⁵⁴ Due to this characters, a number of researches have been evaluated paper based POCT sensors.⁵¹ Fu *et al.* demonstrated two-dimensional paper network format immunoassay card. Lateral flow strip type sensor is coated with the dried reagents and embedded on the card (**Figure 5D**).⁴⁸ Furthermore, paper lengths derived sequential reagent loading, via different flowing time. Through this technique, automatic performance on paper microfluidic system was evaluated. The result is revealed by the matter of visual band, as common strip sensor does, which is easy to check. However, optical detection has a critical issue due to the poor sensitivity so that a number of approaches have been studied to enhance that.⁶⁷ In 2013, Apilux and his colleagues developed an automated paper based sandwich ELISA sensor (**Figure 5E**).⁴⁰ By applying dipropylene glycol methyl ether acetate containing 20% acrylic polymer onto the membrane, patterned channels were fabricated. Following the designed channel, the assay was performed automatically after sample loading. In this study, remarkable consequence about close relationship between fluid flowing time and detection sensitivity was evaluated. More complicated designed channel drew longer duration time and more clear detection results. This study revealed that driven flow rate in porous material is one of the important parameter for performance.⁵⁴ It means that the paper has relatively fast flow rate, it suggests low sensitive sensor, while relatively slow flow rate suggests high sensitive sensor.⁶⁸ Because of this, material selection is very important for paper based microfluidic sensor.

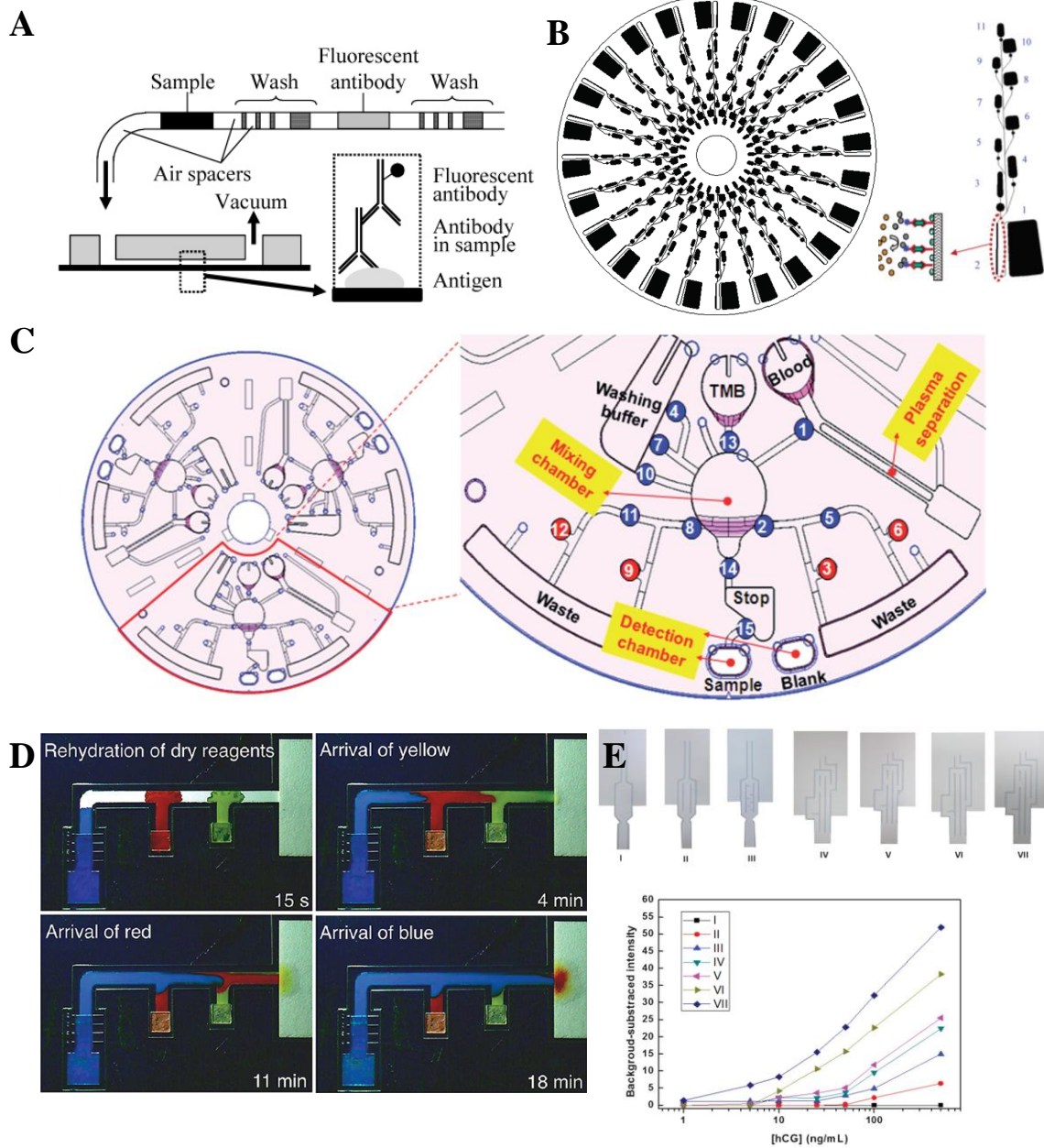


Figure 5. Examples of microfluidics based immunoassay (A) Schematic representation of lab-on-a-chip based immunoassay with prefilled sample in the channel.⁵ (B) ELISA device design with 24sets of assay on one disc.²⁰ (C) Fully-automated immunoassay using lab-on-a-disc.²⁵ (D) Paper based immunoassay cartridge with two dimensional paper networks for serial sample loading.¹⁵ (E) Images of different patterned paper based devices and the color intensity of ELISA results from each patterns.⁴⁰

1.3 Electrochemical Measurement

1.3.1 Chronoamperometry

Electrochemical detection method is a promising technique for POCT system. Since electrochemical detection is not dependent on the optical properties or the turbidity of the biological sample, the device can be made from a wide variety of plastics that are cheaper than cyclic olefin copolymer (COC).^{59, 69} In addition, optical density measurement requires a minimal path length to achieve a desired sensitivity.⁶⁷ However, electrochemical detection measurements can be made on a solution of any size in any sort of vessel. Consequently, electrochemical detection affords smaller assays and, therefore, smaller diagnostic devices. With simple peripheral equipment with low power requirements, it is a great tool for sensitive POCT system.

The basic components of electrochemical sensors are a working electrode, a counter electrode, and a reference electrode that is often combined with the counter electrode to make a two-electrode system. In electrochemical sensors, the reference electrode provides a reference potential to the working electrode to enable the electrochemical cell to operate in a controllable manner. Working and reference electrodes are used to establish a baseline potential, and the counter electrode is used to complete the electrical circuit. In amperometric sensing mode, the current on the working electrode, due to oxidation or reduction of a target species, is measured to detect and quantify the target species.

Amperometry is the measurement of current at a fixed applied voltage. It is performed by applying a step potential to a working electrode in solution and measuring the current generated by electroactive species. When the current is measured over a period of time, this technique is known as chronoamperometry.⁷⁰ To the balanced electrodes, plenty large enough stepped voltage is induced while generating the transition of current. If the (-) stepped voltage is applied to the electrodes staying (+) state, reduction reaction dominates the current signals. Also the current is affected by diffusion velocity from the solution to the surface of electrodes. In the case of two different stepped voltage signals are applied to the electrodes following predetermined time respectively, it is called “double potential step chronoamperometry”. Ultimately, the current i , measured between working and counter electrodes, is a function of the concentration of the target in solution and decreases exponentially with time as described by the Cottrell equation:

$$i = \frac{nFAD^{1/2}C}{\pi^{1/2}t^{1/2}} \quad (\text{Eq. 4})$$

where n is the number of electrode, F is the Faraday's constant, A is the surface area of the electrode, D is the diffusion coefficient of the analyte, C is the concentration of the analyte and t is time.⁷¹ When a large enough voltage is applied to the working electrode, the measured current is directly proportional to the concentration of the target species in the solution.

1.3.2 Chronoamperometric Detection

In terms of the significance of electrochemical detection for medical diagnostics, it makes a more sensitive diagnostic device. More specifically, increasing the sensitivity means that smaller concentration changes of the target will result in larger output signals from the sensor. Furthermore, as the limit-of-detection (LOD) is a function of the sensitivity and the signal stability, increasing the sensitivity improves the LOD.

Electrochemical detection for immunoassay, the species to be quantified electro-activity such that it is able to switch from oxidized to reduced states by losing or gaining electrons. However, compounds that are not electro-active such as proteins can be quantified indirectly when they are coupled with an

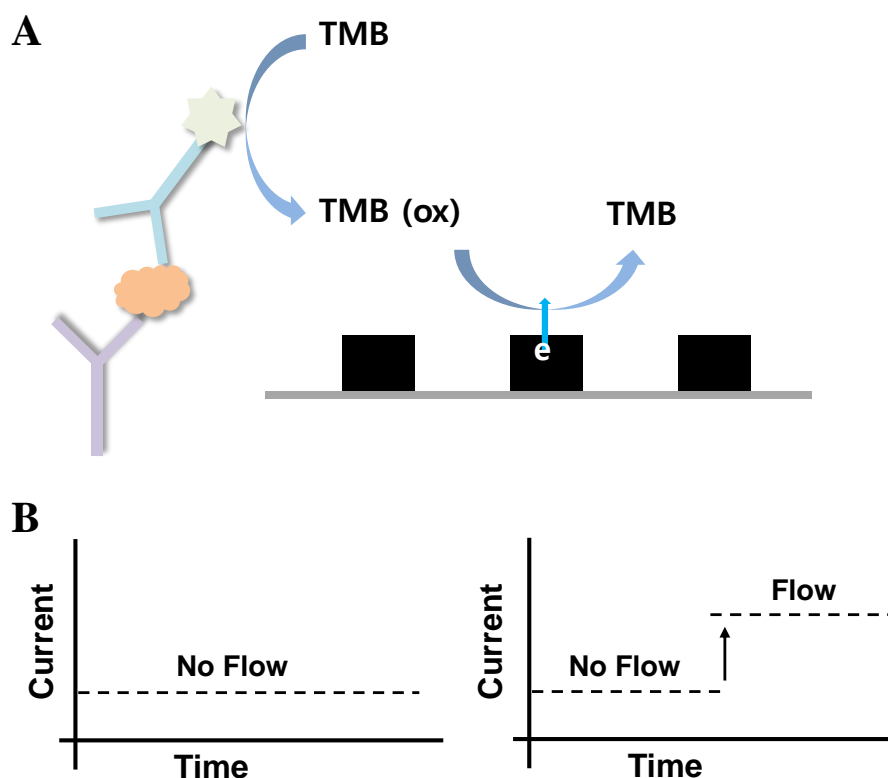


Figure 6. Schematic diagrams of electrochemical measured chronoamperometric signal. (A) The mechanism of electro-active TMB reaction and electrochemical signal reading on the working electrode. (B) Chronoamperometric current signal amplification via fluid flow rate.

ELISA reaction in which the final product such as TMB (e.g., 3,3,5,5'-Tetramethylbenzidine). It can be detected electrochemically in a solution, confirming the presence of the protein. In the ELISA scheme, the enzyme horseradish peroxidase (HRP) enzyme catalyzes the oxidation reaction of the chromogenic substrate, TMB. In the traditional optical ELISA, the absorbance of the oxidation product is measured to determine the concentration of the captured analyte. In case of electrochemical detection, reduction and oxidation reaction of substrate should be coupled. TMB is oxidized during the enzymatic degradation of H₂O₂ by HRP and the oxidized product of TMB has blue color. It is detected by amperometric operation. Both forms of oxidation and reduction of TMB are simultaneously present in the solution. By applying voltage on the electrode, oxidized TMB is selected on the working electrodes, occurring reduction (**Figure 6A**). Theoretically, the measured current on the working electrode is directly proportional to the concentration of enzyme (HRP) immobilized.⁷²

In the case that the solution is flowing over an electrode, the current is a function of the concentration of the analyte and the flow rate, as flow brings more electro-active species to the working electrode's surface, resulting in an increase in the measured current (**Figure 6B**). The limiting current, i , for a planar electrode that is placed parallel to the direction of fluid flow in a channel is proportional to the flow rate in the channel, v , as:

$$i = 1.47nFC\left(\frac{DA}{B}\right)^{2/3}v^{1/3} \quad (\text{Eq.5})$$

where n is the number of electrode involved in the reaction, F is Faraday's constant, C is the concentration of the analyte in the solution, D is the diffusion coefficient of the analyte, A is the surface area of the electrode, and B is the channel height.⁷⁰

1.3.3 Electrochemical Detection based Microfluidics System

In lab-on-a-chip system, Civit *et al* demonstrated a DNA gene detecting device using 16 gold working electrodes array with a silver pseudo reference electrode and a gold counter electrode on a glass slide substrate (**Figure 7A**).¹¹ For the simultaneous detection of two high risk human papillomavirus DNA sequences, TMB-based assay is used to analyze DNA hybridization. Through this, electrochemical measurements for DNA sequences HPV16E7p and HPV445E6 were able to measure to pico-molar scale. Liang *et al.* developed a microfluidic immunoassay system to detect amino terminal pro-brain natriuretic peptides (NT-proBNP) with platinum/Prussian blue nanomaterial (PPN) labeled detection antibodies (**Figure 7B**).²³ After sample incubation, working buffer was loaded to the detection area, where inner removable permanent magnet provided a stable magnetic field. It immobilized magnetic

nanoparticles onto the gold tablet working electrode. Proposed chip has a respectable linearity with the chemiluminescence detection results.

In lab-on-a-disc system blood analysis for glucose lactate or uric acid was studied (**Figure 7C**).²⁶ In this study, gold working electrode, silver/silver chloride reference electrode, and gold counter electrode was used. Especially multi layered carbon nanotubes were integrated on working electrode to improve the accomplishment.

It is clear that electrochemical analysis techniques become popular for immune sensor. Usually, gold material based electrodes are utilized to gain stable signal and high throughput results. However, it has high-cost problem and difficult manufacturing process. It is difficult to develop a general-purpose electrochemical detection based POCT devices with complex fabrication procedures such as photolithography. At this point, advanced technologies with simple fabrication process, low cost material are needed to make commercially available sensitive immune sensor.

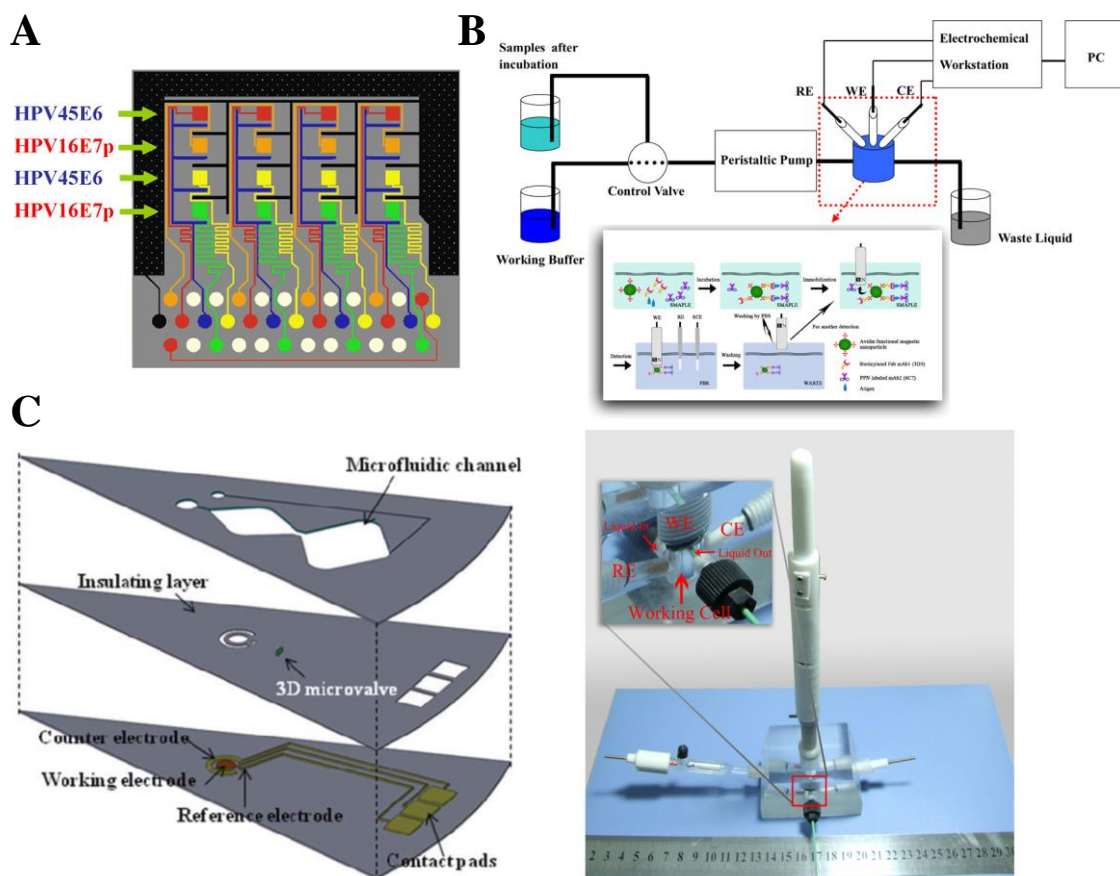


Figure 7. Electrochemical detection on microfluidic system (A) 16 gold working electrodes array to DNA sequencing.¹¹ (B) NT-proBNP targeting immunoassay chip with gold tablet working electrode.²³ (C) blood analysis disc using gold working electrode, gold counter electrode and silver/silver chloride reference electrode.²⁶

1.4 Research Objective

Microfluidic devices could be categorized as lab-on-a-chip system, lab-on-a-disc system and paper-based microfluidics system. Each of them has individual advantages and using that development as real medical diagnostic tools have been actively progressed. Especially, immunoassay system has been widely researched. Based on lab-on-a-disc and paper microfluidics system, there are some commercially available POCT products already. However, to realize an ideal POCT immunosensor, a number of factors must be considered: fully automated, highly sensitive, cost effective, and miniaturized system. Depending on those points, this study suggests two concepts based on lab-on-a-disc and paper microfluidics system.

In chapter 2 “**Lab-on-a-disc integrated with screen printed carbon electrodes for electrochemical detection of protein biomarkers**” cost effective, high sensitive, and fully automated lab-on-a-disc immunosensor is proposed.

- It demonstrated cost effective and easy fabrication process for Screen-printed carbon electrodes.
- It suggested the enhanced amperometric signals by fluid flowing facilitate highly sensitive and stable electrochemical sensor.
- It offered the fully automated ELISA disc integrated with the electrochemical sensor.

In chapter 3 “**Electrochemical velocimetry for real time flow measurement for paper-based microfluidic**” fluid flow of porous-material is monitored. Through this fundamental study about porous material driven flow rate, proper material selection not only for sensitive lateral flow strip sensor but also for other paper based microfluidic devices will be feasible.

- It provided the possibilities of quality control of strip sensor with the information about endemic flow rate of the porous material.
- It evaluated the primary quality of the endemic flow rate depending on the different products, geometric effects, and flow duration with absorption pads.
- It suggested the flow rate modification techniques by applying additional treatment such as oxygen plasma or dextran coating onto papers are studied.

2 Lab-on-a-Disc Integrated with Screen-Printed Carbon Electrodes for Electrochemical Detection of Protein Biomarkers

2.1 Introduction

As mentioned briefly in chapter 1.2.2, early examples of **lab-on-a-disc based immunoassay** devices demonstrated multiple assays sets on a single disc and most of them utilized passive valves such as siphon channel or capillary valve. Siphon channel performs not only fluid blocking but also liquid supplying through rotational speed control. The low RPM generates capillary priming through siphoning channel providing liquid propulsion, while high RPM blocks the flow (**Figure 8A**).⁸ Capillary valve is a type of passive valve utilizing pressure balance between surface tension and centrifugal force.¹³ For example, centrifugo-pneumatic valve is one of capillary valves. It includes air compression effect to enhance closed-valve performance (**Figure 8B**).¹⁷ Through this, closed-valve works well even if the low surface tensional liquid characteristic is filled in channel.

Using these passive valves, various types of lab-on-a-disc systems were developed. In 1999, Duffy *et al.* evaluated a multiple assay disc (**Figure 8C**).¹³ To control the serial transferring of solution through the passive valve, the disc must be rotated with continuously increased speed from 60 to 3000 rpm providing 5nL/s to 0.1mL/s flow rates. Using a single disc, it is possible that simultaneous operation of 48 enzymatic assay sets, which is composed with 3 μ L of 1.0 mg/mL alkaline phosphatase mixture with various concentrations of 3 μ L of theophylline. Likewise, Honda *et al.* developed a column packed simultaneous immunoassay disc (**Figure 8D**).³¹ The column was filled with streptavidin-coated particles for protein modification. A single set of the disc contained 8 connected zigzag-shaped structures. Total 104 sets were integrated in a disc. Using nano-scale sample volume and 50 minutes operation time, carcinoembryonic antigen (CEA) detected as 0.15 pmol/L level. Besides, Morais and his colleagues introduced an indirect micro immune analysis disc by utilizing a sensitive microarray detector (**Figure 8E**).³⁵ The disc consisted of only 1.2 mm thickness of polycarbonate layer coated with aluminum, silver, or gold. For assay, reagents were directly dispensed onto the disc surface. Low reflect (reflection/ transmission: 30/70%) analytical specification allowed a sensitive detection via CD reader laser beam ($\lambda=780\text{nm}$). However, the valve operation, which is related with the burst frequency, is strongly depending on liquids properties and channel geometries. Therefore, reactions with multiple steps are difficult to be integrated and sequentially increased spin speed is required. Furthermore, it is hard to prevent vaporization of liquid via passive valves.

Laser irradiated ferrowax microvalve (LIFM) (**Figure 9A**)⁷ actuated the development of **fully automated ELISA on a disc**. Automation is an essentially required specification to be a POCT device. The LIFM is a representative example of sacrificial valve, composed with 10nm-sized magnetic nanoparticles in paraffin wax. The valve is controlled by simply applying a laser light for a short time (2~10 seconds) to melt the wax at determined position. With biocompatibility and accurate operation, it is suitable to diverse bio-related applications. After the first presentation of the fully automated immunoassay disc from whole blood in 2009,²⁵ Lee *et al.* introduced a simultaneous analysis disc: blood chemistry and immunoassay (**Figure 9B**).¹⁸ For immunoassay, 1mm diameter silica beads coated with 3-aminopropyl triethoxy silane (APTES) were integrated. By applying 3,600 rpm circumvolution for 3min, plasma layer was separated from whole blood and then each metered plasma sample was utilized for blood chemistry and immunoassay respectively. With 350 μ L volume of whole blood, whole processes from sample separation to detection were demonstrated within 22 minutes. The level of performance was equivalent to conventional blood chemistry and immunoassay analysis techniques performance. Additionally, Park *et al.* modified a fully integrated multiplex immunoassay disc (**Figure 9C**).²⁷ In 20 minutes, three analytes (high sensitive C-reactive protein (hsCRP), cardiac troponin I (cTnI), and N-terminal B-type natriuretic peptide (NT-proBNP) were detected from whole saliva sample. It was the first demonstration of the automated and multiplexed immunoassay disc. Through these studies, disc based ELISA technologies developed on the level of fully automated procedures. Most of them, optical detection (OD) is used as a sensing method due to the simple and easy operation. However, it has shortcomings to be POCT devices because of intricate total measurement system and relatively low sensitivity.

Electrochemical detection on a disc garnered an interest recently. It is a high sensitive and selective sensing method, even providing the simple operation. Moreover, electrochemical sensors can be easily miniaturized, facilitating micro- and nano- scale integration. Based on electrochemical method, there are various studies. In 2011, Noroozi *et al.* presented an electrolysis-induced pneumatic pressure pump integrated in a disc system (**Figure 10A**).⁶ Electrolysis was utilized for the pneumatic pressure from aqueous solution and then it caused the propulsion of sample in an upstream direction was generated, against a rotating disc. By using planar gold electrodes, electrochemical based pumping, gating and metering of liquids in a disc were evaluated. In 2013, Abi-Samra and his colleagues evaluated an electrochemical velocimetry effect (**Figure 10B**).²² To measure electrochemical signals on a rotating disc, an electrical slip-ring was mounted onto the spin motor and it was connected to a peripheral potentiostat. By using the printed circuit board (PCB), electrical contact was stably generated between the slip-ring and the gold electrodes. As the flow rate increases, the chronoamperometric current signal was increased. Based on this study, Kim *et al.* developed a fully

integrated ELISA disc with electrochemical detection under rotating state (**Figure 10C**).³⁰ The miniaturized gold electrodes on a glass substrate were embedded into the disc. With flowing state measurement, amperometric current was enhanced. Due to the amplified current, much enhanced sensitivity was gained.

Though the electrochemical detection makes the highly sensitive immunoassay devices, most of electrochemical sensing based studies are depending on the gold electrodes. To make miniaturized gold electrodes, optimized MEMs process is necessary and it requires the manageable substrate such as glass for gold printing, which is hard to integration into micro system due to the fragile characteristic. However, for POCT tool, inexpensive components and easy fabrication procedures are very important to be widely used and manufactured. Therefore, in this study, **research objective** is focused on the development of chip, easy to make and high sensitive ELISA device. Via screen-printed carbon electrodes and flow-enhanced signaling effect, fully-integrated ELISA disc is evaluated.

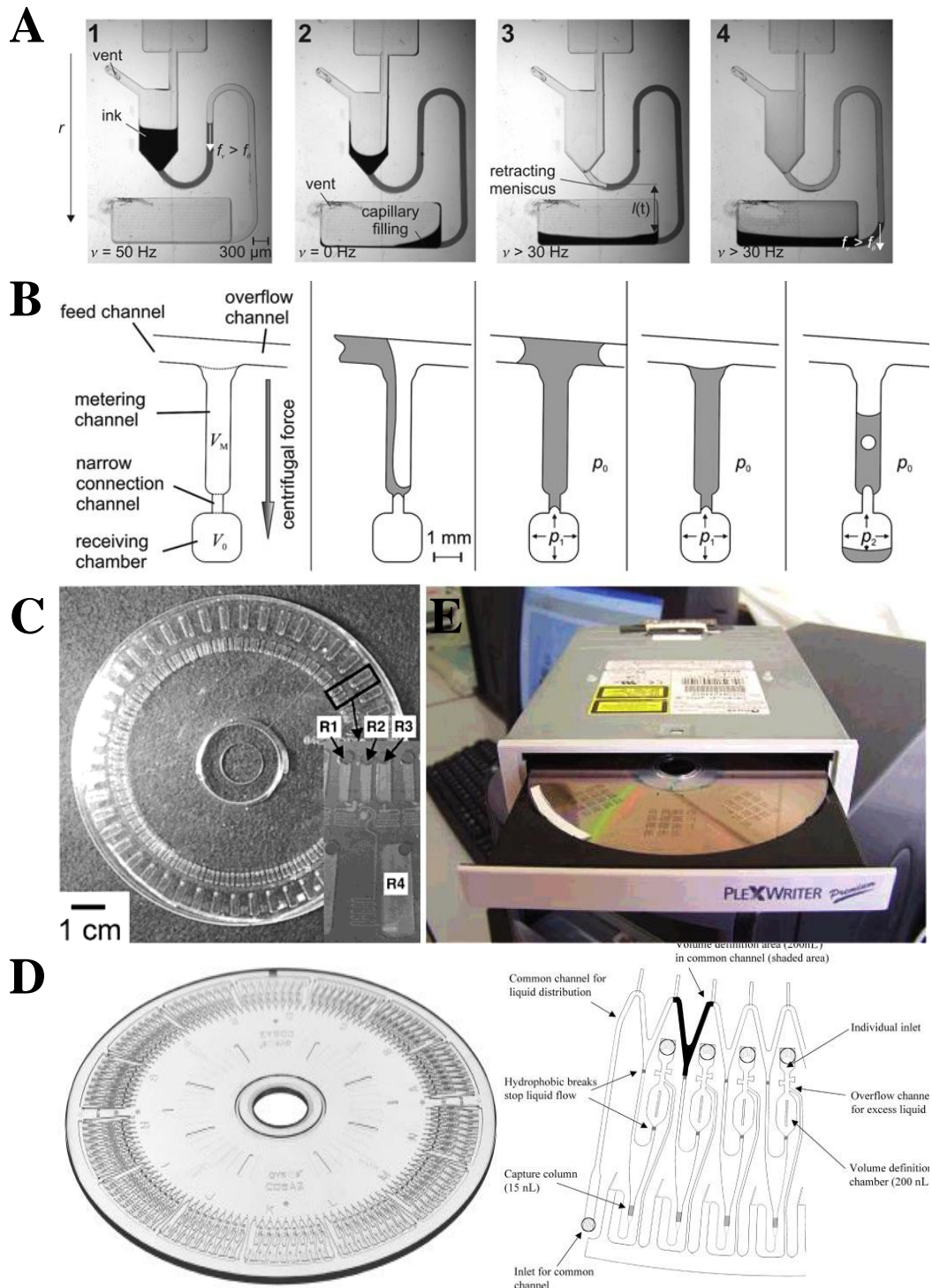


Figure 8. Simultaneous multiple operation lab-on a disc based immunoassay. (A) Siphon channel structure and valve working.⁸ (B) Centrifuge-pneumatic valve, which is an example of capillary valve.¹⁷ (C) Multiple enzymatic disc with capillary passive valve.¹³ (D) Column packed simultaneous multiple assay disc.³¹ (E) microarray based protein analysis compact disc.³⁵

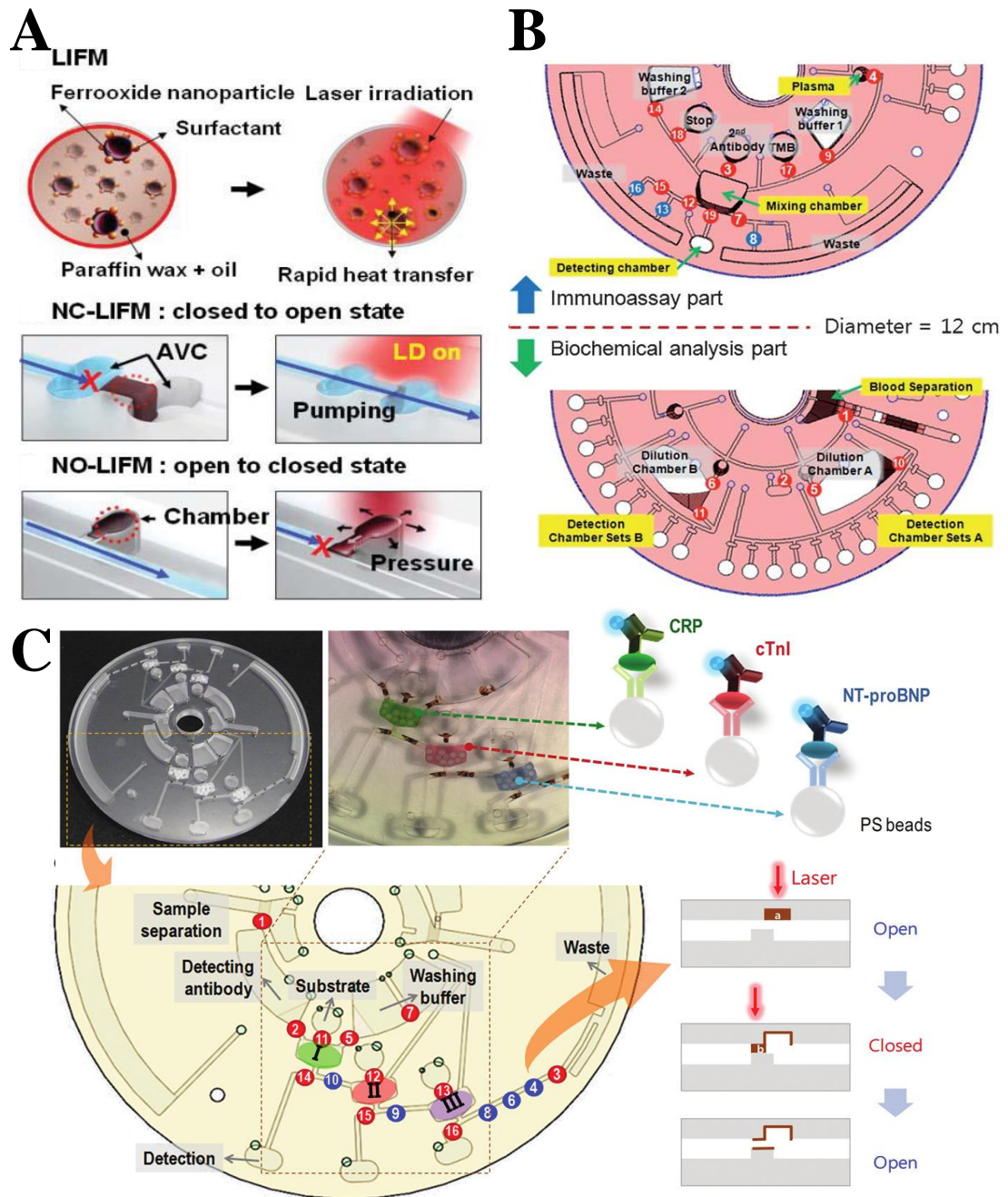


Figure 9. Examples of fully automated ELISA on disc. (A) Schematic design of laser irradiated ferrowax microvalve (LIFM) operation.⁷ (B) Simultaneous blood chemistry and immunoassay analysis disc.¹⁸ (C) Fully integrated multiple immunoassay disc.²⁷

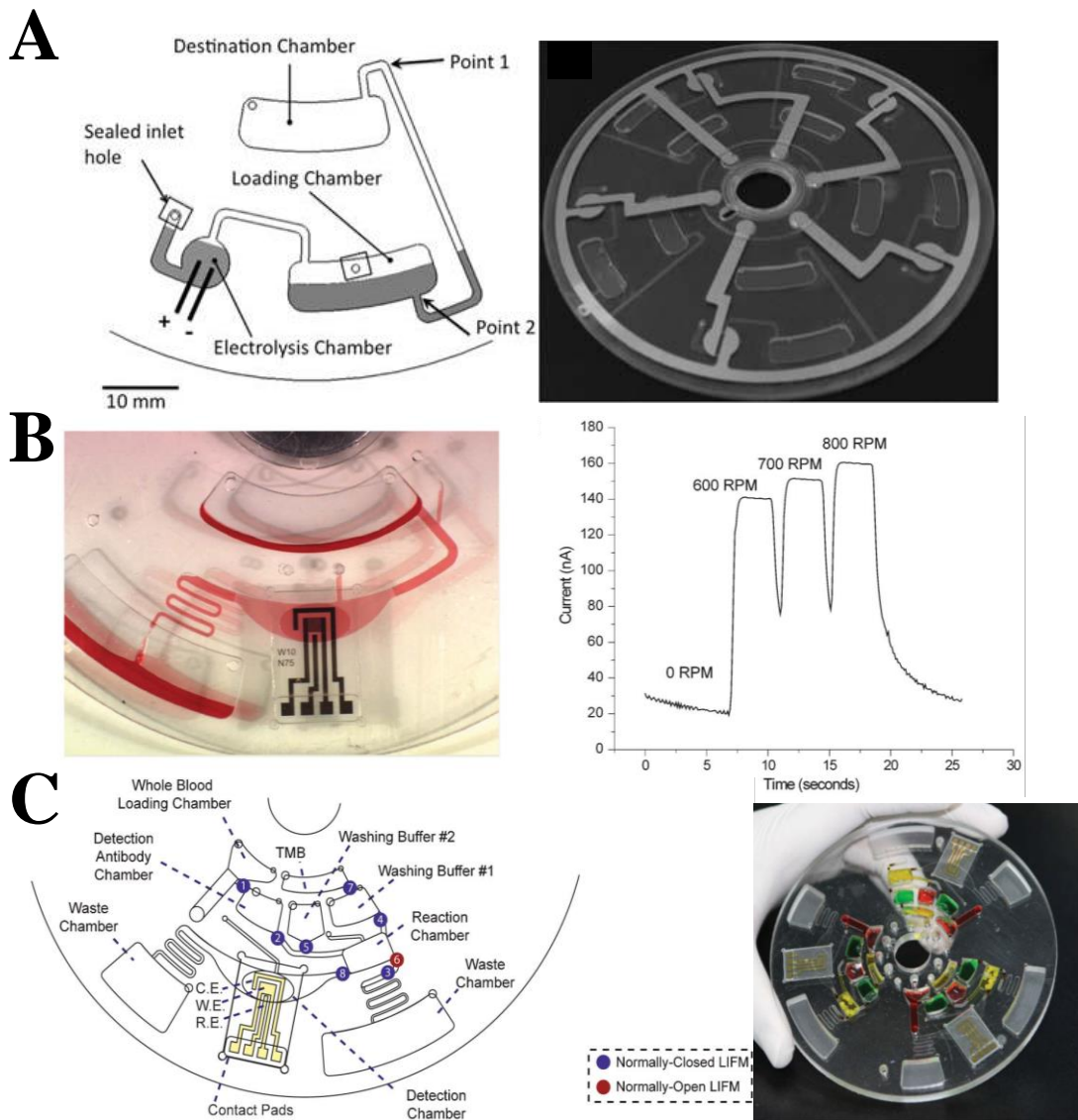


Figure 10. Examples of electrochemical sensor integrated lab-on-a-disc devices. (A) Electrolysis based pneumatic pressure pumping disc.⁶ (B) A study about enhanced electrochemical signal derived by fluid flow on a disc.²² (C) Electrochemical detection based fully integrated ELISA disc.³⁰

2.2 Materials and Methods

2.2.1 Reagents

Immunoassay

As capturing antibodies, monoclonal mouse anti-human hs C-reactive proteins (clone # C5, Hytest Ltd., Finland) in a coating buffer (20 μ g/ml in 100 mM Bicarbonate/carbonate, pH 9.6; Junsei Chemicals Co., Ltd., Japan) were used. Horseradish peroxidase (HRP) conjugated goat polyclonal anti-high sensitive C-reactive proteins (hsCRP; 200ng/ml; Abcam plc., MA) were utilized as detection antibody to detect hsCRP (Abcam plc., USA) in PBS. 1 % BSA/1X PBS (99 % purified Bovine Albumin, Bio Basic Inc., Canada) was used as blocking solution, and 0.1 % BSA/1XPBS buffer was accepted as washing buffer. The TMB solution (AbD serotec, UK) was managed as substrate without additional modification. The stop solution dissolved in 0.2 M sulphuric acid (Matsunoen Chemicals Ltd., Japan) was prepared.

Electrolyte solution

For electrochemical performance evaluation, **electrolyte solutions** of 5 mM ($[\text{Fe}(\text{CN})_6]^{4-}$) (Sigma-Aldrich) with 250 mM KCl (Junsei Chemical Co., Ltd., Japan) in PBS was prepared and used to test the electrodes. Chronoamperometric recordings were generated using its proprietary software (EC-Lab Software v.10.02 BioLogic, France).

2.2.2 Fabrication of Screen-Printed Carbon Electrodes

Materials

Carbon screen-printed electrodes (SPCEs) were printed on the 0.125mm thickness of polycarbonate (PC) sheet. As shown in **Figure 11A**, the miniaturized electrode fitted onto an 11mm by 14.5mm PC sheets. The electrode had an effective surface area of the working electrode to be around 8 mm³. The designed projected mask was designed on polyimide tape (AM00000068, 3MTM with DuPontTM Kapton[®], USA). Whole electrode body including working and counter electrode parts was composed with carbon paste (C2000902P2, Gwent Inc., UK). For reference electrode part, silver/silver chloride (Ag/AgCl) paste (011464, BAS Inc., Japan) was applied.

Fabrication

SPCEs were consisted with working electrode, counter electrode, and reference electrode. A negative mask was created according to a desired design cut by the plotter (Graphtec CE 3000-60 MK2, Graphtec, USA). To print the electrodes, the mask was applied to a clean substrate at first. Since it

was important to have a good contact between the mask and the substrate, a single-sided adhesive for the mask was securely attached to the substrate. Carbon paste was simply applied through the mask by pushing the paste into all of the features of the mask, and the excess was removed. After that, carbon paste was allowed to dry. Ag/AgCl paste was dropped onto the reference electrode part. Then, the mask was peeled or removed off from the substrate (**Figure 11B**).

2.2.3 Fabrication of lab-on-a-Disc

Milling of polycarbonate layers

The top layer was made of 1mm thickness of polycarbonate (PC) and the bottom layer is made of 5mm thickness of PC layer, separately. Computer Numerical Control (CNC) micromachining (3D modeling machine; M&I CNC Lab, Osan, Korea) fabricated microstructure on both PC plates by milling. The top layer had inlet holes and dispensing holes for ferrowax valve, while the bottom layer had storage chambers and channels (**Figure 12**).

Ferrowax valve

The dispensing holes on the top plate were filled with injected ferrowax. Ferrowax was composed

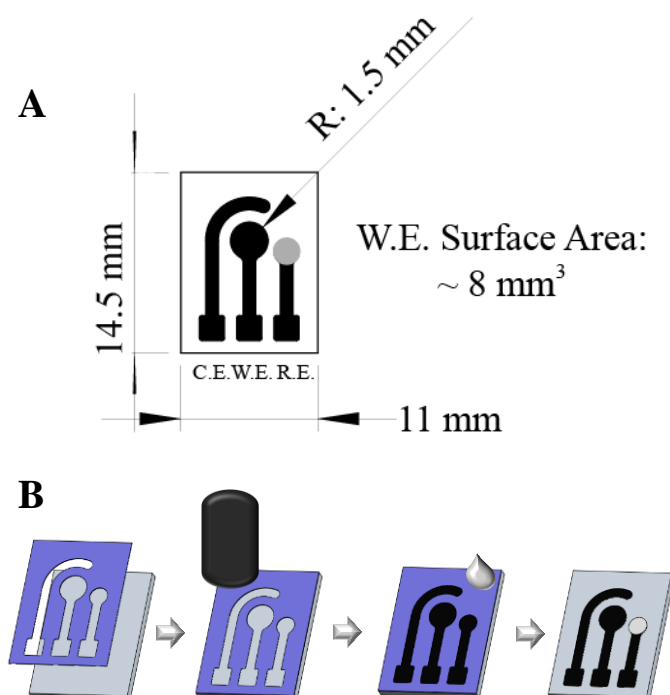


Figure 11. Fabrication of screen printed carbon electrodes (SPCEs). (A) Detailed design of SPCEs and the size of each part. (B) Fabrication process of SPCEs: mask assembling, carbon paste loading, Ag/AgCl paste loading for reference electrode, drying and mask removal.

with 50% of paraffin wax (T_m 50-52 °C, Fulka Chemine, GmbH) and 50% of ferrofluid (APG 314, Ferrotec Inc, CA, USA). By using a wax dispensing machine (Hanra Precision Eng. Co. LTD., Incheon, Korea), spontaneously controlled volume of molten ferrowax was dispensed to determined position on heated top plate automatically.

Capturing antibody immobilization

Ten polystyrene beads (2mm diameter, Hoover, USA) were coated with primary antibody on its surface and then the beads were integrated into the bottom layer's reaction chamber on disc. To compare conventional assay performances, 96 well-plate (96 Well Clear Flat Bottom Polystyrene High Bind Microplate, Corning Inc., USA) was prepared.

Lab-on-a-disc assembling

SPECs were embedded onto bottom layer within a 0.1mm height of detection chamber of the disc. There were two double-sided pressure sensitive adhesive tapes (Flexmount DFM 200 Clear V-95 150 Graphtec, USA) for SPECs integration and channel fabrication between the top and bottom PC parts (**Figure 12**). One adhesive layer covered the SPECs to isolate on bottom layer. After then, the circumferentially-orientated microfluidic channel designed adhesive layer was entrenched. This channel design enables the electrodes to be fully covered by liquid solution without any bubbles or air pockets when liquid was transferred from the reaction chamber.²² Finally, all of the 2 adhesive layers and two PC layers were pressed through pressing machine to assemble (Mechanical Power Vise AVQ-160GHV, Auto Well Enter Co., LTD., Taiwan).

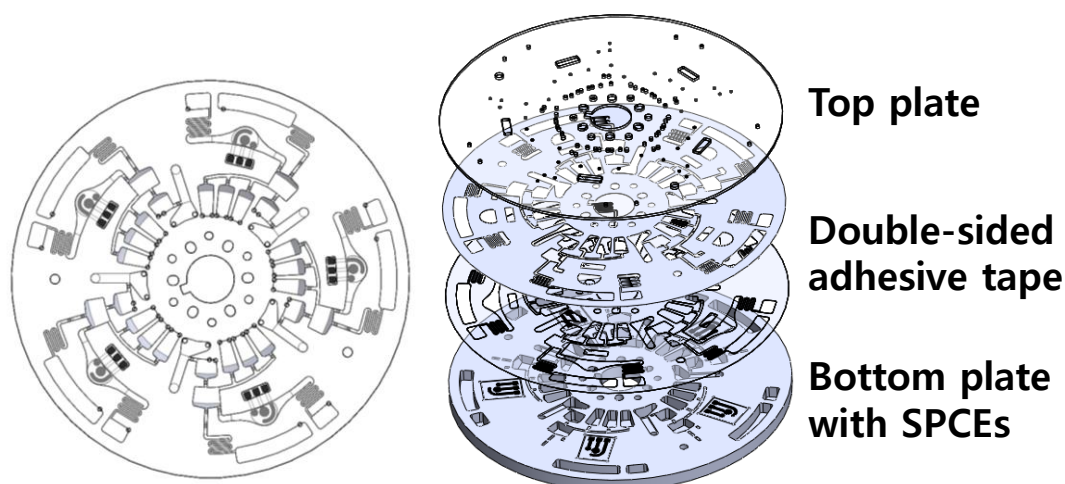


Figure 12. Schematic design of lab-on-a-disc for electrochemical detection integrated with SPCEs and the exploded illustration of the disc.

2.2.4 Measurement System

Motion and visualization system

The motion system was composed with rotor, laser stage, magnet stage and controller. The rotor was purchased by Yaskawa Electric (SGMIV-02A 200W servomotor, Japan) and it was possible to rotate up to 6000 rpm. With charge coupled device camera (CCD digital color camera; IK-TF5C, Toshiba, America, Inc., USA), sequential images during disc operation were taken as programmed speed and intervals. From Opto Electronics (Chongqing Co., China), laser (808nm High-Power Laser Diode AL808T3000) was bought. It could move by X-Y axis stage and it had 3W power to control open/close the valve.

Electrochemical measurement system

As shown in **Figure 13**, printed circuit board (PCB) was a component for the electrical connection between the electrodes embedded within the microfluidic disc to the electrical slip-ring. A single sided copper PCB layer was a 1.5mm thickness and 124 diameter board. It had two kinds of pins for connection. One was dowel pin for electrical slip-ring, which was composed with copper (McMaster Carr, USA, 97325A121). The other was gold contact pins for electrodes, which was purchased from Mouser Electronics (USA, Mouser Part, 575-906115). Electrical slip-ring was composed with a spin chuck and an electrical slip-ring. The spin chuck was mounted onto the spinning motor and holds the whole system. It was composed with the 3D CNC milled aluminum part and plastic insulator parts. The plastic insulator supported the microfluidic disc mechanically and isolates electrically from the conductive spin chuck with the rest of the system. Electrical slip-ring part (Fabricast, inc, 2511 Seaman Ave. South EI Monte, CA 91733) transferred electrical connection to the rotating systems. It had 6 channels and contact pins (Mouser Electronics, USA, 818-100804-002). By using the peripheral potentiostat (Model: VSP, BioLogic, France), it was possible to make continuous electrical contact during rotation. Chronoamperometric recordings were generated using its proprietary software (EC-Lab Software v.10.02 BioLogic, France).

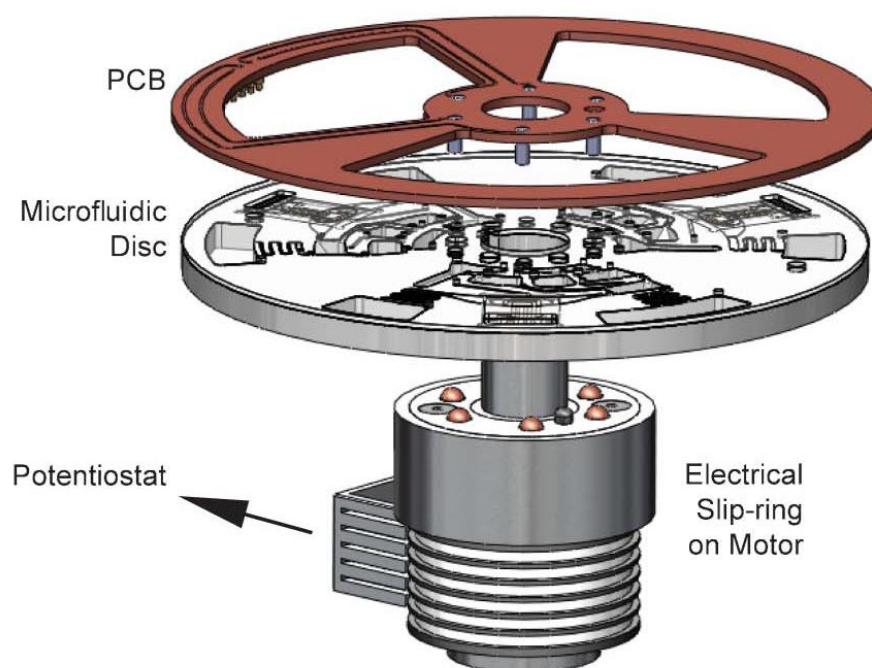


Figure 13. Electrochemical measurement system for the rotating lab-on-a-disc. It is composed with PCB to make electrical contact between electrode and disc, microfluidic disc to assay process and detection, potentiostat to make continuous electrical contact during rotation, and electrical slip-ring on motor to transfer stationary electrical connection to rotating system.

2.3 Results and Discussion

2.3.1 Electrodes Performance

Optimization for screen-printed carbon electrodes

Screen-printed carbon electrodes (SPCEs) are commonly used in industry (e.g. glucose test strip) since they are relatively easy to fabricate and low in cost. The technology is straightforward. Through a mask, carbon paste is deposited onto a substrate and dried to form solid electrodes. For fabrication, substrate can be a variety of insulating materials. To evaluate the feasibility using SPCEs on various substrates, some substrates are tested with carbon paste. The results from the evaluation of screen-printing the carbon paste onto these substrates are briefly summarized in **table1 (p.41)**. Polyvinylidene fluoride (PVDF) membrane, polycarbonate (PC), and paraffin wax blocked cellulose (paper) have been identified as suitable substrates for screen-printing carbon electrodes in terms of penetration. Because the reproducibility of electrode fabrication is important if the electrode volume (or surface area) varies from device to device, then the diagnostic result will also vary. Among various substrates, PVDF membrane and PC have been identified as the best substrates as the carbon paste do not bleed on or through the material after application. Through this experiment, the electrodes can be screen-printed directly onto the PC microfluidic disc material that is easy to integrate. Also, the surfaces of air dried carbon electrode at room temperature and 60°C oven dried carbon electrode are observed by scanning electron microscope (SEM) photograph and through this, 60°C for 30minuets oven drying condition is accepted (**Figure 14**).

After optimizing the drying conditions for the carbon paste fabrication, signal stabilization is evaluated. The oxidation and reduction peaks shift along the applied voltages depending on the electrochemical oxidation and reduction rates at the interface of the working electrode, which are determined by many factors, such as electrode material, surface conditions, and solution pH. Therefore, cyclic voltammetry is an indispensable step to evaluate the optimal operational condition for electrode. By applying Ag/AgCl paste for the reference electrode, signals become much stable. In **Figure 15A and B**, the electrodes without reference part show unsteady results. Those figures show very different graph profiles despite all electrodes have same design, fabrication technique, and measurement condition. It is evident of inconsistent sensing performance. On the other hand, in **Figure 15C and D**, the reference electrode is added to the carbon electrode, resulting in much enhanced stability and reproducibility of signal. Even the electrodes fabricated separately, they show quiet same signal profiles, which means greatly consistent performance from electrode to electrode. With the optimized conditions for carbon electrodes, the coefficient of variance (CV) of 10 electrodes is less than 5% from the cyclic voltammogram of 10 electrodes with very similar performances

overlapping curves. As a result, included an Ag/AgCl reference electrode improves signal stability drastically.

Electrochemical performance

In order to demonstrate the sensing performance, chronoamperometric signals are measured relying on a range of different concentrations of electro-active solution: potassium ferrocyanide ($[\text{Fe}(\text{CN})_6]^{4-}$) of 10, 5, 1, 0.2, 0.1, 0.01, and 0 mM. To figure out the electrodes' accomplishment, the commercially ordered products by a supplier (KTPtech, Korea), which has same geometric structure, are tested with same method and condition. Overall, the lab-made SPCEs and the commercially fabricated electrodes are tested correspondingly across the concentration ranges. The black line shows the current derived by lab-made SPCEs and red line shows the results of commercially ordered product's signals. Both electrode types have a coefficient of variation (CV) less than 4 percent. As shown in **Figure 16A**, lab-made SPCEs have higher results in current values than commercially ordered one via whole concentrations. The limit of detection (LOD) in 3times standard derivations (3SD) is $2.67\mu\text{M}$ and $0.371\mu\text{M}$ for lab-made and commercial product, respectively. In conclusion, both lab-made and commercially fabricated electrodes are very reproducible.

Table 1. Summary of the results from the evaluation of screen-printing carbon paste onto various substrates: definition of printing and penetration into material.

<i>Substrate</i>	<i>Result of Carbon Paste on Substrate</i>	
	<i>Definition</i>	<i>Penetration</i>
Polyvynylidene fluoride membrane	Excellent*	No
Nitrocellulose membrane	Okay*	Yes
Cellulose	Okay	Yes
Cellulose blocked with paraffin wax	Okay	No
Polycarbonate	Excellent	No

*Excellent = Paste stayed within defined mask region

*Okay = Paste bled on the substrate by approximately 0.1 ~ 0.5mm because of wicking.

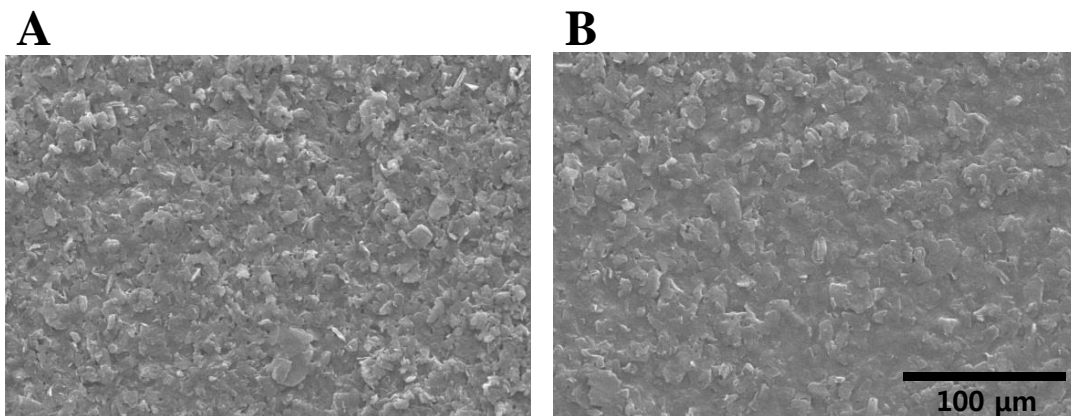


Figure 14. SEM photographs of the surface of a carbon electrode. (A) The surface of air dried carbon electrode at room temperature. (B) The surface of oven dried carbon electrode at 60 °C.

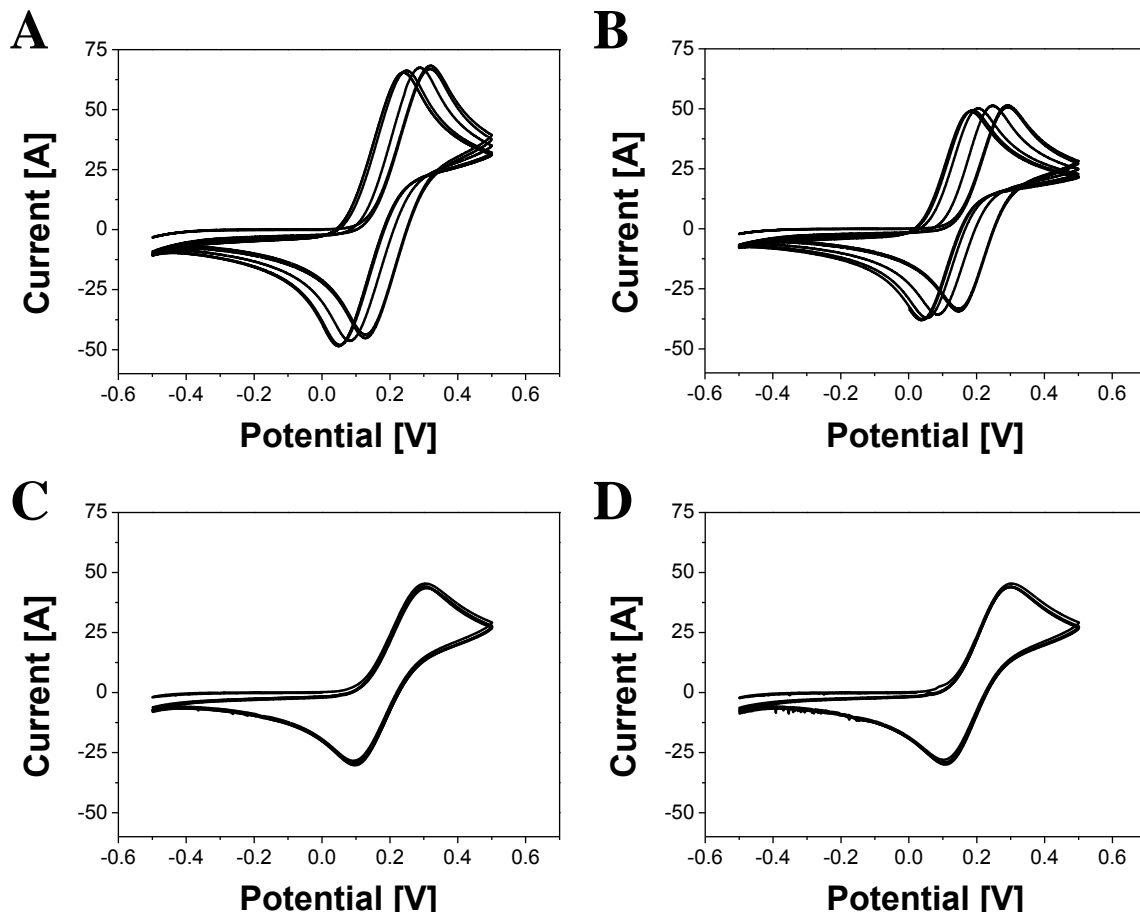


Figure 15. Reference electrode addition results with cyclic voltammograms. (A, B) When there is no real reference electrode, the signal is very unstable, evident by the shifting cyclic voltammograms, furthermore, there is no reproducibility from batch to batch. (C, D) Reference electrodes (Ag/AgCl) are added to the electrode set, significantly stabilizing the signal and thus the cyclic voltammogram. Electrode stability is also revealed from batch to batch.

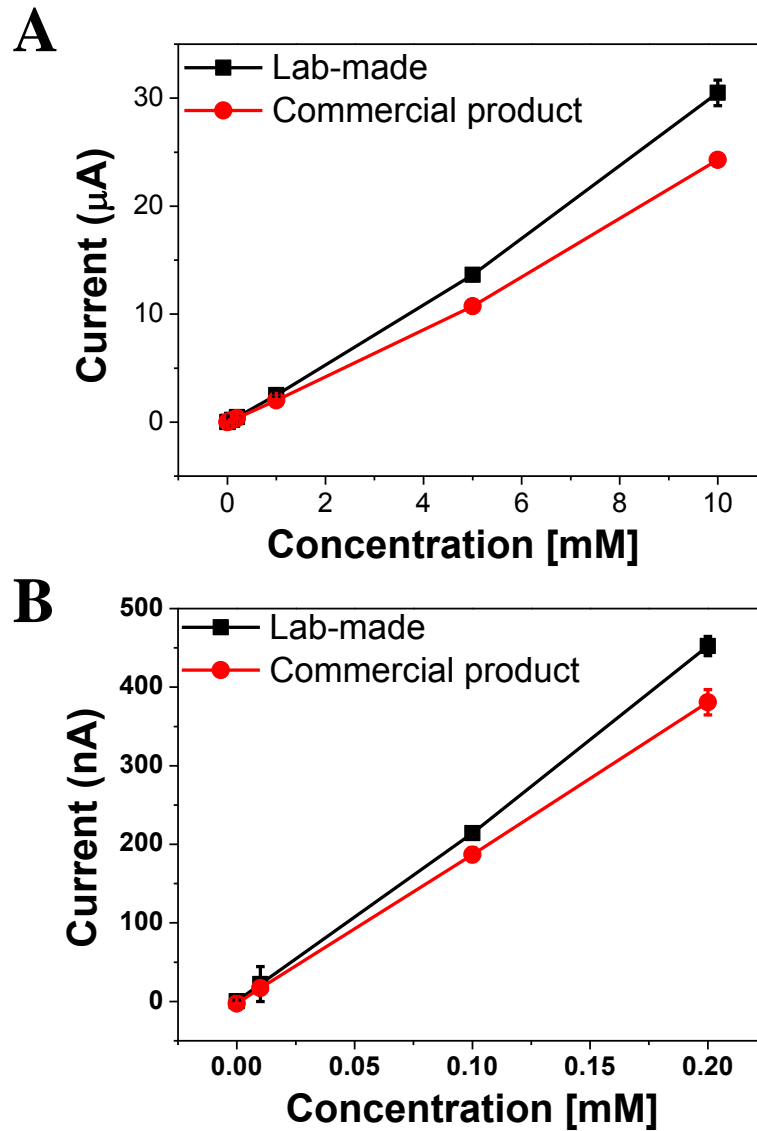


Figure 16. Electrode performances of lab-made SPCEs and commercially ordered product SPCEs. (A) Amperometric results with entire concentration from 0~1.0 mM electro-active solution. (B) Zoom in the plot between 0~0.2 mM electro-active solutions.

2.3.2 Disc Operation

Immunoassay

The disc is composed with sample loading chamber, detection antibody chamber, reaction chamber, washing chamber, TMB substrate storage chamber, waste chamber, detection chamber, and connecting channels. In addition, there are 7 normally-closed valves and 1 normally-open valve. Numbers on valve position means the operation order (**Figure 17**). The C-reactive protein (CRP) spiked in PBS sample (150 μ L) is loaded into the sample collection chamber. After separation and metering, 75 μ L of supernatant solution is brought to the detection antibody chamber by opening the valve #1 (**Figure 18B**). After the mixing step of the transferred sample with 75 μ L of the detecting antibody solution (200 ng/mL) for 10 seconds under acceleration of the disc shaking, valve #2 is open by laser emitting to move the mixed solution to the reaction chamber, which has primary antibody-coated polystyrene beads. For incubation of antigen/secondary antibody, the disc is shook for 10 min (**Figure 18C**). By opening valve #3, the extra solution is washed out to the waste chamber. Serial washing steps to wash away excessive reagents is followed twice. Then, through open the valve #4 and #5, each washing step has shaking for 20 seconds (**Figure 18D**). After then, normally open valve #6 is closed to control the flowing direction of substrate to the detection area. Valve # 7 is open to transfer TMB solution to the reaction chamber, and then, incubate for 5 min with shaking (**Figure 18E**). Finally, the reacted-substrate mixture is moved to the electrodes by opening valve #8. **Table 2** shows the detailed spin operation that programmed.

Electrochemical detection

For the electrochemical detection, -0.2 voltage is applied to measure chronoamperometry. There are two different detection modes: stationary and rotation. Stationary detection mode operates at 0 RPM, while flowing mode operates on rotational disc at 400 RPM (**Table 2**) resulting in flowing-enhanced amperometric signal.³⁰ Electrochemical detection is measured for 35 seconds at the stationary mode, and for 15 seconds at the flowing mode to maintain the fixed volume of substrate.

Table 2. Operation programs of lab-a-disc device for fully automated immunoassay with electrochemical detection.

<i>Spin No.</i>	<i>Valve No.</i>	<i>Time (s)</i>	<i>Operation</i>
1			Sample loading
2	1	10	Sample transfers to detection antibody chamber and mixing
3	2	600	Incubation with antibody-immobilized polystyrene beads
4	3		Remove extra solution
5	4, 5	40	Washing 2 times
6	6		Close the valve
7	7, 8	5	Priming to detection part
Stationary detection			0 RPM
Flowing detection			400 RPM

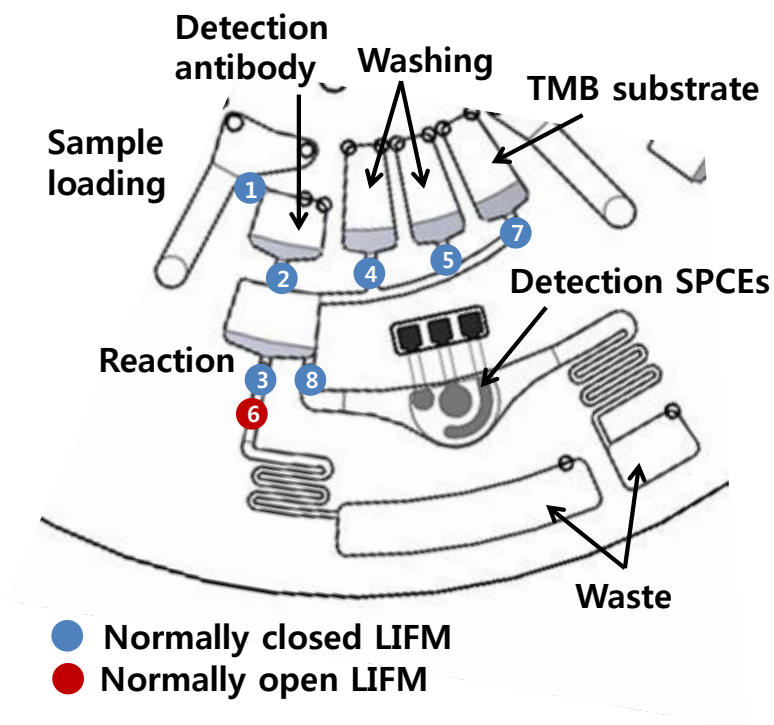


Figure 17. Detailed illustration of SPCEs integrated microfluidic disc with valves. It is composed with sample loading, detection antibody, reaction, washing, TMB, and waste chambers. There are 7 normally closed LIFM valves and 1 normally opened LIFM valve.

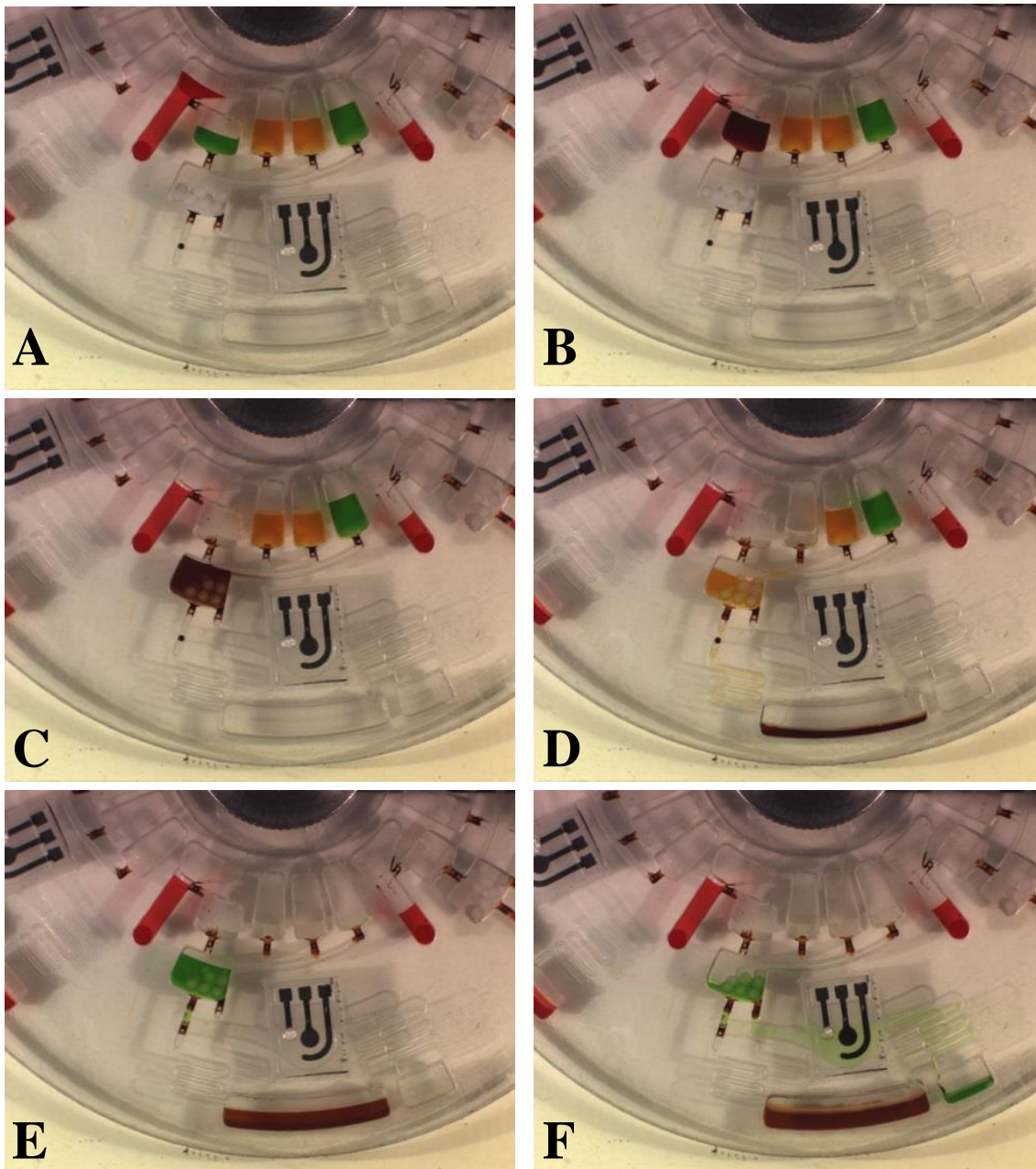


Figure 18. Operation of centrifugal microfluidic disc with color dyed water. (A) Loading CRP spiked sample and separation. (B) Metering of sample to transfer onto detection antibody chamber and mixing for 10s. (C) Mixed sample with detection secondary antibody is moved to reaction chamber, which is integrated to capturing antibody coated 10 polystyrene beads. And then, the sample is incubated for 10 minutes with shaking. (D) Excess sample is washed away to waste chamber, and then twice of serial washing is operated for 40 s each. (E) Substrate, TMB, is loaded to reaction chamber, and incubated for 5 minutes. (F) Reacted TMB solution is primed to SPCEs detection part. No rotation is occurred for stationary detection, while flowing detection takes place with rotation at 400rpm.

2.3.3 Diagnostic Performance

Stationary mode detection

One of the critical concerning when switching from gold electrodes to carbon paste electrodes is the diagnostic performance regarding to the limit of detection and sensitivity, which is the most important point to make useful POCT device. Typically, gold has a lower resistance with higher charge transfer rate and acts as a more sensitive sensor in comparisons to a carbon-based electrode which has a lower charge transfer rate. To evaluate the diagnostic performance of SPCEs based electrochemical detection, a range of concentrations of CRP in PBS is demonstrated; the concentrations tested are 0, 1, 2.5, 5, 12, 25 ng/mL of CRP and detection via chronoamperometry with -200mV. Electrochemically quantified a full automated ELISA assay results are detected using gold electrodes and carbon electrodes and the signals are compared as shown in **Figure 19A**. Overall, it is clear that the gold electrodes give higher signals for all the concentrations of CRP at stationary station. However, carbon electrode shows relatively good performance even with the great differences of price and fabrication process. The limit of detection is corresponding to 3 times the standard deviation (3SD). The mean value of the blank sample for the experiments quantified with carbon electrodes and gold electrodes are determined as 263.6 pg/mL and 202.1 pg/mL respectively. It is caused by the increased surface area of SPCEs, which is 30 percentages bigger than the gold electrodes. Briefly, the limit of detection (LOD) for both sensor types (gold and carbon) is turned out to be fairly similar even with stationary mode measurement as shown in **Table 3**.

Flowing mode detection

As flow brings more species to the electrode's surface, the detection performance become better, while providing increased sensitivity and ultimately improved LOD. The fluid flowing is generated by centrifugal spinning at 400 RPM. Overall, the LOD measured as 59.24 pg/mL in SPCEs, which is a 4.5 times improvement over the LOD for stationary measurements via SPCEs (**Figure 19B**). As shown in table 3, flowing mode carbon electrode has a favorable reproducibility. In addition, carbon electrodes showed much enhanced sensitivity even higher than gold electrodes under flowing mode detection.

Optical detection

To do the comparison of the diagnostic performance between electrochemical measurement and quantified ELISA assay measured by optical density (OD) detection is gained simultaneously (**Table 3**). Assay process is operated as exactly same as on-disc assay experiments, only except the final detection method. To check the OD results, the reacted TMB is transferred to the conventional 96-

wellplate. The LOD (3SD) for the OD is determined to be 115.66 pg/mL, which is certainly higher than SPCEs based measurement.

As a result, flow generated by rotation gives a great advantage for diagnostic performance even with cost effective SPCEs, which have worse characteristics for electrochemical sensor than gold material based electrodes. So SPCEs with flowing measurement show 3.41 times better sensitivity than stationary gold electrodes. Also, Ag/AgCl reference electrode effectively works producing stable signaling, which is resulted in the lowest average coefficient of variance value around 4 percentages (**Table 3**).

Table 3. Results of ELISA by electrochemical detection with different detection methods: carbon electrodes at stationary mode, carbon electrodes at flowing mode, gold electrodes at stationary mode, optical detection.

<i>Detection method</i>	<i>LOD (3SD) [pg/ml]</i>	<i>Signal to Noise ratio (S/N ratio)</i>	<i>Average Coefficient of Variance (%)</i>	<i>Coefficient of Variance at 1ng/mL CRP (%)</i>
Carbon Stationary	263.6	9.8	9.75	5.4
Carbon Flowing	59.24	16.9	4.02	6.2
Gold Stationary	202.1	12.9	7.53	7.1
Optical detection	115.66	34.5	6.01	6.64

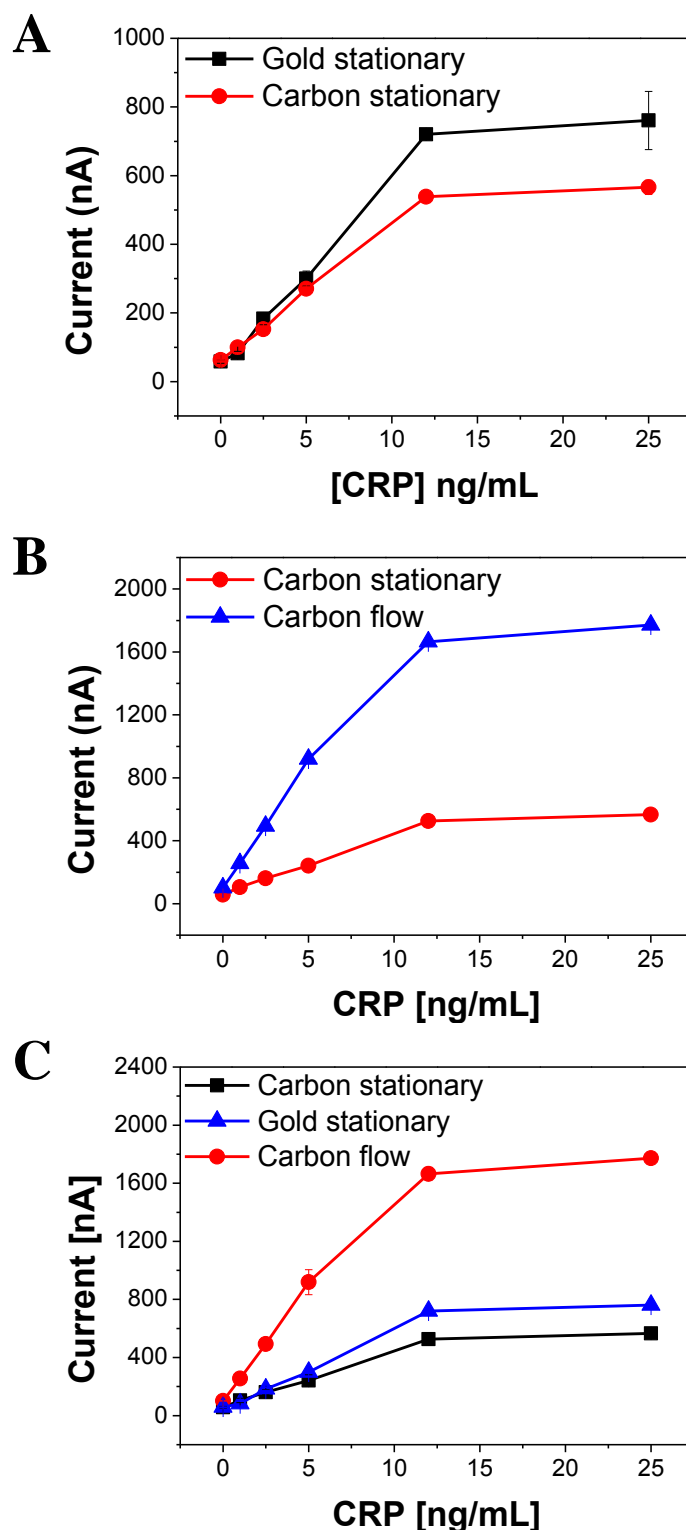


Figure 19. On-disc electrochemical immunoassay's calibration curved obtained by different detection methods. (A) Assay results with carbon electrodes and gold electrodes at stationary mode. (B) Evaluation of flow-enhanced signaling effect with carbon electrodes. (C) Assay results with carbon electrodes at stationary mode, carbon electrodes at flowing mode and gold electrodes at stationary mode.

2.4 Conclusion

After the demonstration of ELISA technique on microfluidic system, there are evolutionary developments in this field. From the simultaneous multiple assay disc to fully automated assay disc, various researches are studied. Furthermore, the way to overcome some limitations of previous optical detection method, electrochemical measurement is introduced recently; however, gold material and MEMs fabrication process have expensive cost problem and complicated manufacturing product. It gives a difficulty of integration of electrochemical detection into the real POCT system.

In this study, cost effective, easy to fabricate and high sensitive screen-printed carbon electrodes (SPCEs) based fully-automated immunoassay disc is invented. The reproducibility of lab-made SPCEs is compared to commercially ordered product, and the results show very comparable performance of lab-made SPCEs. Even the carbon based electrodes have generally less sensitive due to the material characteristic than gold electrodes as an electrochemical sensor, fluid flowing enhances the amperometric current signals and then it is possible that cheap and high throughput detection sensor development. Through this, SPCEs based immunoassay disc has lower limit of detection than the stationary state gold electrode's measurement.

3 Electrochemical Velocimetry for Real Time Flow Measurement for Paper-Based Microfluidics

3.1 Introduction

After the first advent in late 1940's,^{73, 74} paper-based microfluidics has recently garnered significant interest in POCT societies due to some advantages of paper: affordable, robust, and equipment free operation. Most of all, paper is a very low cost material so that it could offer diagnostic devices at an unprecedentedly low price compared to other microfluidic based POCT tools.⁴⁴ Furthermore, porous structure of paper determines capillary-driven passive transferring of fluid without any external pumping source and it could be an answer of portable POCT devices applying compatibility with chemical, biochemical, and medical applications to the resources limited countries.^{48, 49}

Practically speaking, **paper based immunoassay sensor** is widely used as POCT tool in these days.⁵¹ As shown in **Figure 20**, there are a number of examples of commercially available paper-based immunoassay sensor products. The most popular and familiar lateral flow strip sensor is human chorionic gonadotropin (HGC) pregnancy test kit. **Figure 20A** is one example of HCG test kit. It provides the early detection of pregnancy by visual band within 5 minutes using urine sample.³ AlereTM developed a human immunodeficiency virus (HIV) test kit (**Figure 20B**).¹⁰ Inside the cover, strip sensor is embedded. Through whole blood sample and chase buffer loading, both the HIV-1 p24 antigen and HIV-1/2 antibodies are detectable in 20 minutes. Another ensample is malaria test kit. Malaria is one of the difficult diseases to diagnose due to the misjudgment with typical flu-like symptoms. However, immunoassay based lateral flow strip sensor can support the malaria diagnosis accurately (**Figure 20C**).¹² Especially, malaria is popular in the developing countries so cost effective paper based POCT devices is very helpful. Also, influenza A+B test kit, which requies three handling steps to test, is developed as strip sensor type.¹⁹ Furthermore, not only diseases diagnosis but also beta-agonist drugs test is available by using paper based immunoassay sensor in these days.²⁴ Overall, paper based microfluidic devices has capillary force as the only driving source and there is an inverse proportional relationship between flow rate and detection sensitivity of strip sensor.⁵⁴ Therefore, the intrinsic flow rate of each paper materials is the most critical parameter for assay performance.

It is a powerful tool for health care disease screening⁵⁰ as well as for **other applications**: environmental analysis, food quality test,⁷⁵ portable solar cell,⁷⁶ fuel cell or battery,^{29, 34} or drug test.²¹ For example, there is a study about paper fluidics depending on dimensional properties.⁹ As shown in **Figure 21A**, three-dimensional (3D) paper system was demonstrated. By applying the programmed

fluid dynamics on paper, it was able to evaluate the chemical signal amplification with simultaneous sample flowing, and automated biological assay. This concept was based on capillary driven flow of paper and the flow rate is an important variation. Weaver *et al.* demonstrated a fast paper screening analytical devices (PADs) for pharmaceutical quality test using paper microfluidic system (**Figure 21B**).²¹ Utilizing the capillary action of paper, pharmaceutical components were brought to the hydrophilic test line. The reaction in each lane generated color bar code, which can easily recognize in visual. To indicate the best intensity signals, the optimization of flow rate was the most critical issue due to the different reaction time among the samples. For example, the starch and iodine showed rapid decaying rate, while the talc and eosin red showed slow appearance speed. In 2013, meanwhile, Fraiwan and his colleagues introduced a paper based microbial fuel cell (**Figure 21C**).²⁹ This device was composed with a paper based proton exchange membrane (PEM), patterned paper with hydrophobic wax to generate a reservoir, anode layer, and sample input layer. Once a sample was dispensed into the device, current was generated immediately. However, the signal decreased in 10 and 15 minutes due to the permeation time and flow duration time. Likewise, indium-doped tin oxide (ITO) electrodes integrated paper-based electrochemical sensor (**Figure 21D**) to analyze glucose had a decreased signal after 5 minutes as same reason.³⁴ These portable power supplier systems in paper microfluidics have significant parameters from porous material's flow rate and duration time.

So **studies for flow rate measurement on porous material**, which exhibits capillary-driven flow such as paper or fabric, has been explored. Typical flow rate monitoring technique, particle image velocimetry (μ PIV), is shown in **Figure 22A**.¹ In this method, particles in fluidic are captured by laser and it became visualized. It is useful to monitor the continuous state fluid by using a lattice scale. But, it has complicated detection system, which is not enough to integrate micro- or nano- scale devices. Recently, some researches have introduced to monitor and measure the flow rate of paper through visual observation via camera images. In these kinds of studies, perceivably distinguishable color dyed water is absorbed by a porous materials to monitor the flow mechanisms. In 2011, geometric effect of paper to flow rate was observed.¹⁵ The tracer species were loaded to three varying widths of strips as shown in **Figure 22B**. In detail, a phenol red in phosphate-buffered saline generated color change to fuchsia as a band shape under pH control by using electrode. The relative transferring time of tracer species are evaluated depending on the widths of the strip. Fu *et al.* developed the two-dimensional paper networks system and they demonstrated the programmed flow by analyzing optical images (**Figure 22C**).⁴⁸ To trace fluid flow mechanism and the distance proceeded by fluid, color dyed water was loaded into paper. Through this technique, the effect of paper width and the delaying time are revealed by using dissolvable barrier. Kauffman *et al.* suggested a technique to measure the flow rate via small volume of liquid by applying either photo-activation or electrochemical activation

(Figure 22D). A certain portion of the solution was decorated with dye, and the displacement of the dyed solution was monitored over time of paper wicking. The photograph showed a remarkable band of liquid flowing in the paper and the information was determined by consecutive framed images.

Overall, visual observation to modify paper-fluidics has been widely used, while there are some drawbacks due to the separated analysis process: duration time, image analysis, and the flowed distance measurement upon nonhomogeneous curvature structured flowing profile. Also, the poor resolution derived by concomitant effects of dye solution's diffusion offers inaccurate results. It means there is yet a velocimetry monitoring technique for paper that is both easy to use and provides detailed flow information. Therefore, in this study, **research objective** is a development of paper fluidics monitoring system via electrochemical sensor, which is easy, cheap and highly accurate.

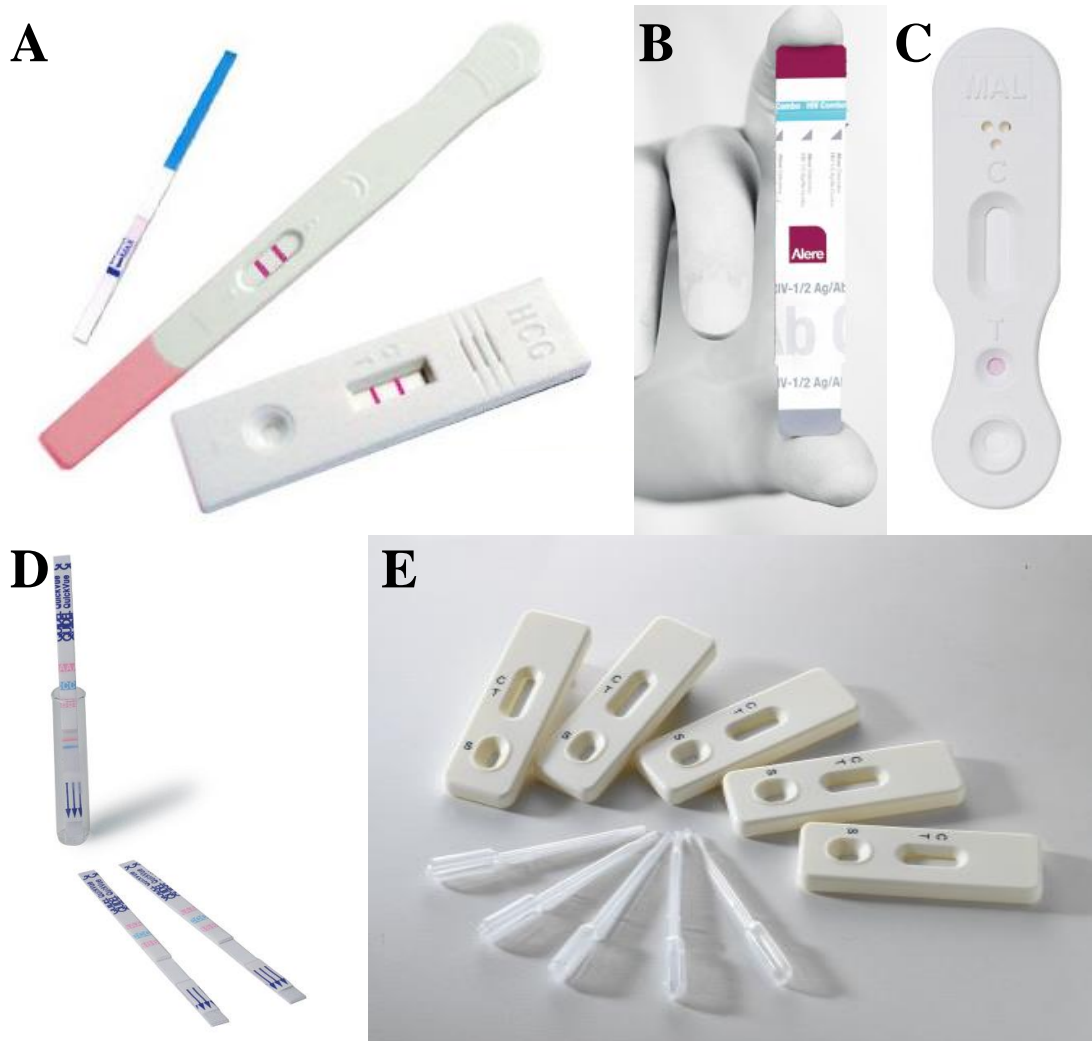


Figure 20. Paper or porous material based commercially available diagnostic lateral flow strip sensors. (A) HCG pregnancy rapid test kit.³ (B) Alere Determine™ HIV-1/2 Ag/Ab combokit.¹⁰ (C) Malaria rapid test kit.¹² (D) The QuickVue Influenza A+B tests kit.¹⁹ (E) Beta-Agonist (Clenbuterol) rapid test kit.²⁴

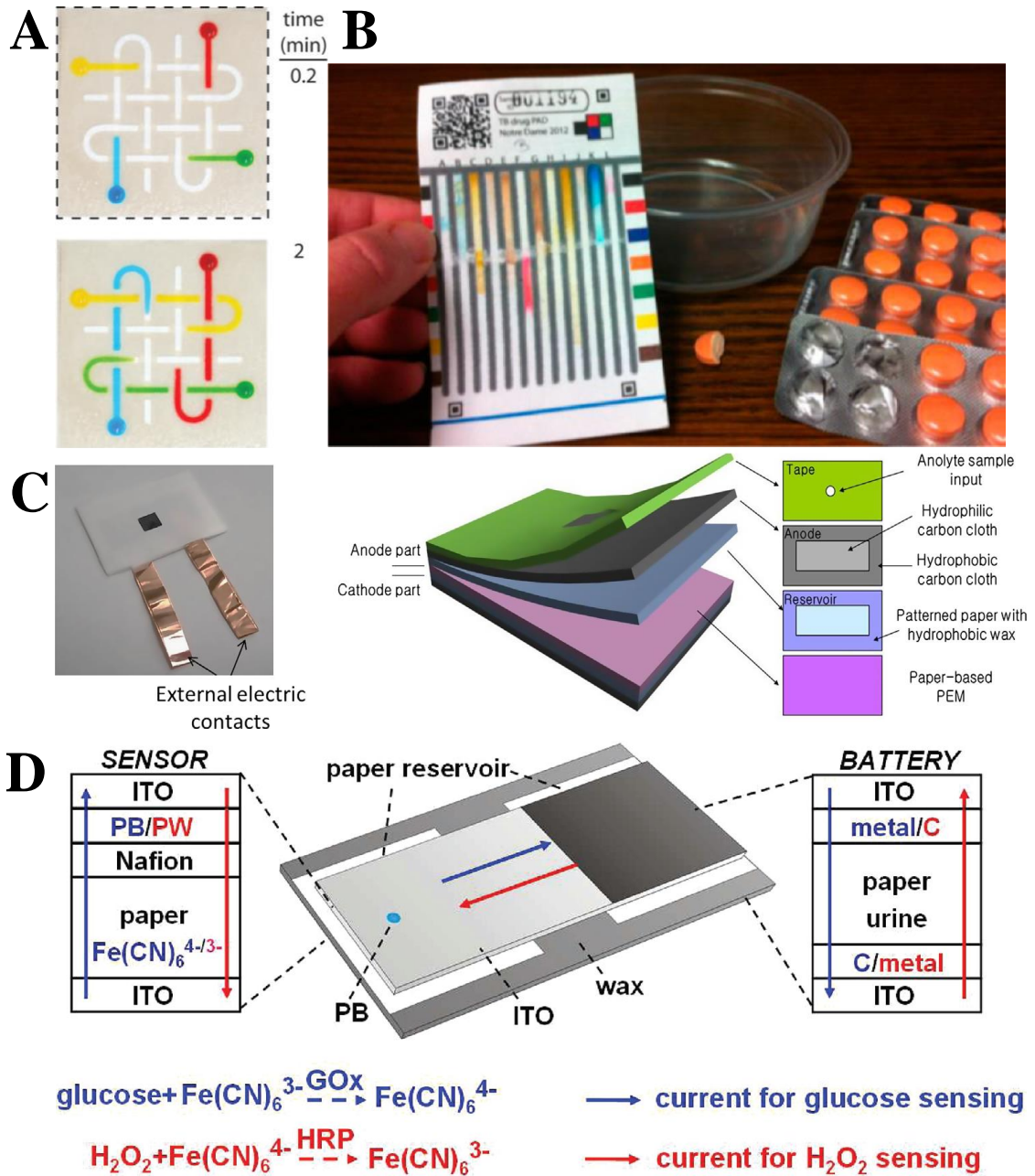


Figure 21. Applications of paper microfluidic system besides diagnostic test kit. (A) Three dimensional paper network to control progress order of fluid flow in the system.⁹ (B) Drug component analysis paper card.²¹ (C) Paper based portable microbial fuel cell.²⁹ (D) Portable paper electrochemical sensor with ITO battery.³⁴

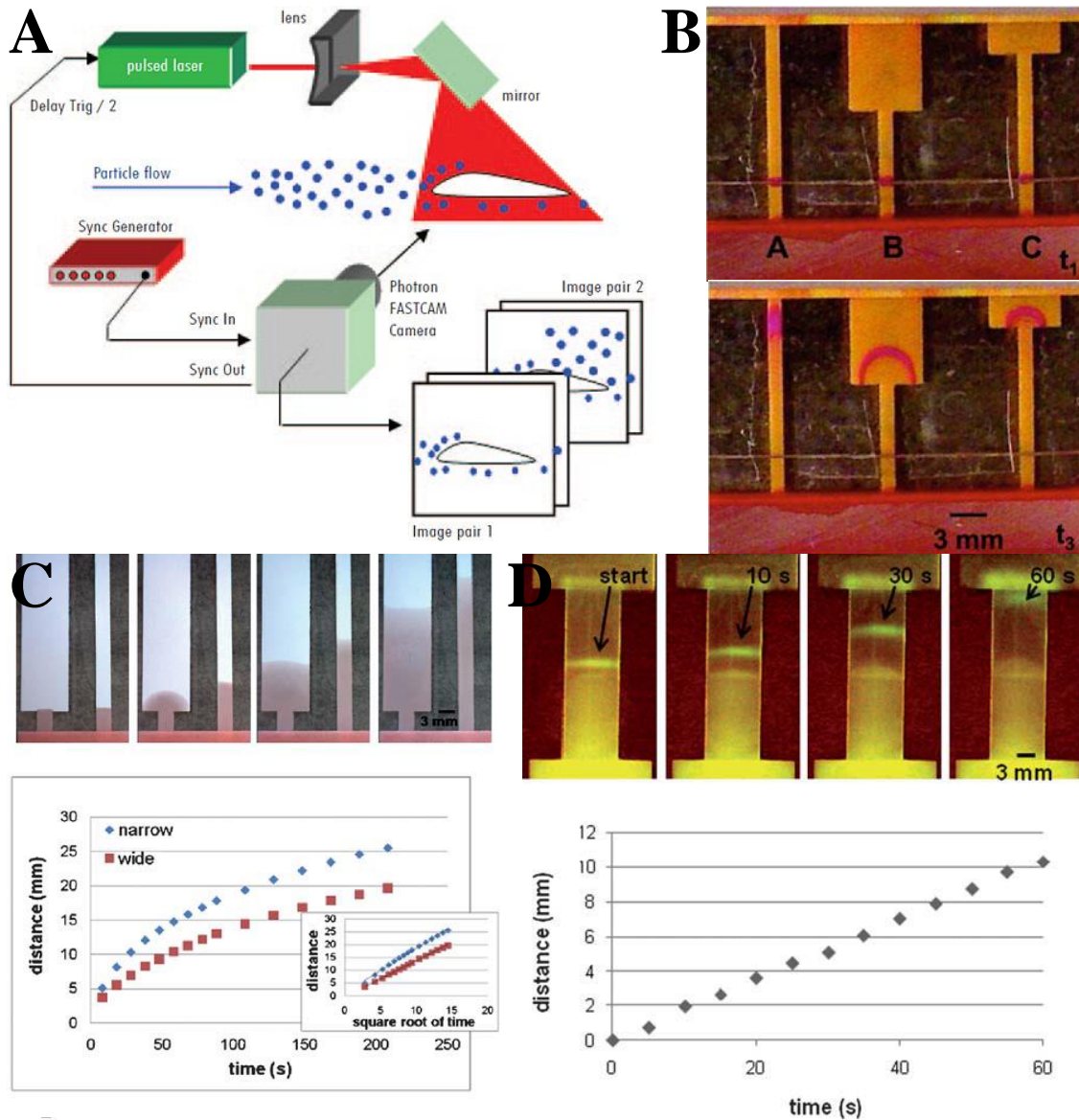


Figure 22. Current techniques to measure paper fluidics flow rate based on optical detection. (A) A schematic diagram of micro particle image velocimetry.¹ (B) Tracer species based fluid flow measurement under specific pH.¹⁵ (C) Fluid flow measurement with food color dyed water.²⁸ (D) Flow monitoring technique using the change of optical property of small volume of liquid by applying either photo-activation or electrochemical activation.

3.2 Materials and Methods

3.2.1 Reagents & Materials

Paper samples

Paper strips were obtained from Pall Corporation (Absorbent Pad 111 & 133, Vivid 170 Nitrocellulose; Pall Corporation, USA), and Whatman TM (Filter paper 4; Whatman TM, UK). Those samples were cut to size with a paper-cutter (Smart Cut A445; Rexel, England). The dimensions of the paper were verified by a digital caliper (Vernier calipers, Nanoto) and all paper samples had a tolerance of ± 0.1 mm. Nitrocellulose was modified either by oxygen plasma treatment or dextran solution (DEX). Oxygen plasma was performed on Nitrocellulose strips by a vacuum plasma system (Model: Cute-MP, FEMTO Science, South Korea). It was treated with 50 sscm condition for 1 minute. Solutions of DEX were prepared separately by addition 12% w/v DEX T500 (MW: 500,000, Pharmascosmos, Denmark) to buffer solutions. The DEX solutions were applied on the NC strips via a fine brush and allowed to dry at ambient temperature for min prior to the experiment.

Electrolyte solution

For experimentation, electrolyte solutions of 10 mM $[\text{Fe}(\text{CN})_6]^{4-}$ (Sigma-Aldrich) with 250 mM KCl (Junsei Chemical Co., Ltd., Japan) in PBS were prepared and used within several hours after preparing. The electrodes embedded in the device were consociated to a potentiostat (Model: VSP, BioLogic, France) and chronoamperometriy was performed via proprietary software (EC-Lab Software v.10.02 BioLogic, France).

3.2.2 Device Fabrication

Screen-printed carbon electrodes

SPCEs were consisted with working electrode, counter electrode, and reference electrode. A negative mask was created according to a desired design by cutting plotter (Graphtec CE 3000-60 MK2, Graphtec, USA). A single-sided adhesive (AM00000068, 3MTM with DuPontTM Kapton[®], USA) for the mask was securely attached to the substrate. Carbon paste was simply applied through the mask by pushing the paste into all of the features of the mask, and the excess was removed. After the drying, Ag/AgCl paste was dropped. After the second drying as same condition as carbon paste was dried, the mask was peeled or removed off from the substrate.

Microfluidic device

The device was fabricated using top-down techniques by Computer Numerical Control (CNC) micromachining (3D modeling machine; M&I CNC Lab, Osan, Korea). The device wa composed

with polycarbonate (PC) layers milled by CNC micromachining and double-sided pressure sensitive adhesive layers (DFM 200 clear 150 POLY H-9V-95, FLEXcon, USA) cut by tape-cutting plotter (Graphtec CE 3000-60 MK2, Graphtec, USA) automatically (Figure 23A). In detail, 1mm thickness of PC for device sustention, 0.125mm thickness of PC for electrode printing, and 5mm thickness of PC for reservoirs were used. All of separated parts were assembled by a pressing machine (Mechanical Power Vise AVQ-160GHV, Auto Well Enter Co., LTD., Taiwan) (**Figure 23B**).

3.2.3 Measurement System

Neglecting the gravity effect, pressure depending on Darcy's law in porous media with Newtonian liquids was the only driving force of this system:

$$Q = \frac{KA}{\eta L} \Delta P \quad (\text{Eq. 6})$$

$$Q = \text{flow rate} \left(\frac{m^3}{s} \right),$$

$$K = \text{permeability coefficient} (m^2),$$

$$L = \text{thickness of test sample} (m),$$

$$A = \text{area of cross - sectional area to flow} (m^2),$$

$$\eta = \text{fluid viscosity} (Pa \cdot s)$$

When the surface tension from the outlet portion of channel is considered as a resistance of flowing, the net driving pressure by media insertion is given by

$$\Delta P = \Delta P_c - \gamma \left(\frac{1}{R_x} + \frac{1}{R_y} \right) \quad (\text{Eq. 7})$$

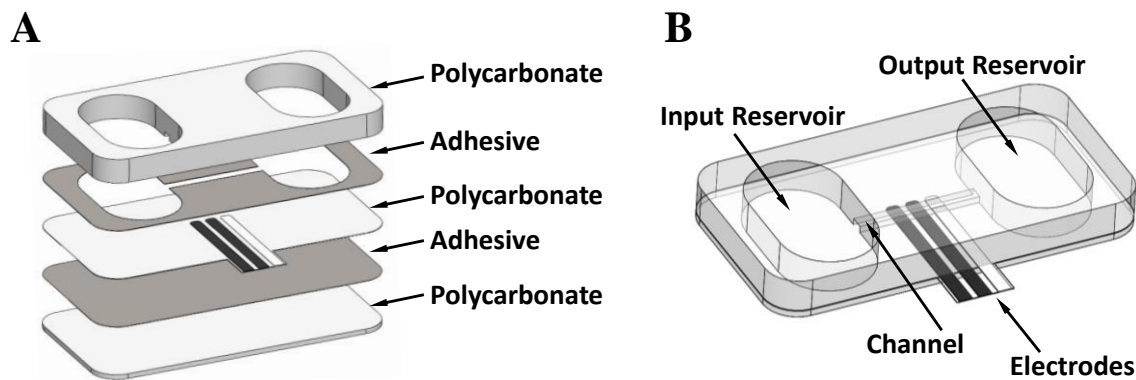


Figure 23. Schematic illustration of device. (A) Exploded view of device, which is composed with polycarbonate layers and pressure-sensitive adhesive layers. (B) Fabricated device with two input and output reservoirs, and SPCEs accommodated connecting channel between two reservoirs.

where γ is the surface tension of the fluid and R_x and R_y are radii of curvature in each of the axes parallel to the surface. If the channel width and thickness are W and H , R_x and R_y could be expressed

$$R_x = -\frac{W}{2\cos\theta} \text{ and } R_y = -\frac{H}{2\cos\theta} \quad (\text{Eq. 8})$$

By applying water solution properties and the initial flow rate approximately 100 μ l/min, which was driven by nitrocellulose membrane; it is possible to calculate the degree of surface tension curvature.

The permeability coefficient of Vivid nitrocellulose membrane was studied.⁷⁷ The end point value of positive delta pressure condition, occurring capillary-driven flow toward the device, informed applicable channel geometry; with the fixed length as 20mm, the height of channel must be bigger than 0.25mm. Withal experimental evaluation, 1mm for channel height was adapted due to differences between reality and assumption of liquid properties with electrolytes, gravity effect, and mass of fluid.

Overall, each reservoirs of the device had 1.5mL volume capacity. Geometry of connecting channel was 2 mm width, 1 mm height and 20 mm length. The inserted electrochemical sensor contacting channel was fabricated by screen-printing carbon paste (Gwent Group, UK, Product: C2000802P2) and silver/silver chloride (Ag/AgCl) paste (ALS, Japan, Product: 011464) onto a 0.125mm thickness PC substrate.

3.2.4 Electrochemical Velocimetry Converting Method

Whole device was filled with electrolyte solution: inlet, outlet reservoirs, and connecting channel. Through the potentioestat attached electrodes integrated channel inside, chronoamperometric electrochemical detection was occurred as base line at first. After the signal becoming stable, a strip was introduced to the outlet reservoir, resulting in the fluid flow; when the strip was dipped into liquid filled reservoir, solution was sucked up via capillary force, generating fluid flow in the connecting channel (**Figure 24**). By using the peripheral potentiostat, chronoamperometric recordings were generated using its proprietary software.

Flow rate driven by porous material could be calculated from electrochemically measured results using a theoretical equation. The limiting current, i , measured by the electrode is related to the average volumetric flow rate, v , as:

$$i = 1.47nFC\left(\frac{DA}{B}\right)^{\frac{2}{3}}v^{\frac{1}{3}} \quad (\text{Eq. 9})$$

where n is the number of electrodes, F is Faraday's constant, C is the concentration of the analyte, D is the diffusion coefficient, A is the area of the electrode, and B is the channel height.⁷⁰ The device presented in this study has properties of $n = 1$, $F = 96,485.3365 \frac{C}{mol}$, $C = 10mM$, $A = 4mm^2$, $B = 1.5mm$ and $D_{ferrocyanide} = 0.65 \cdot \frac{10^{-5}}{cm^2s^{-1}}$

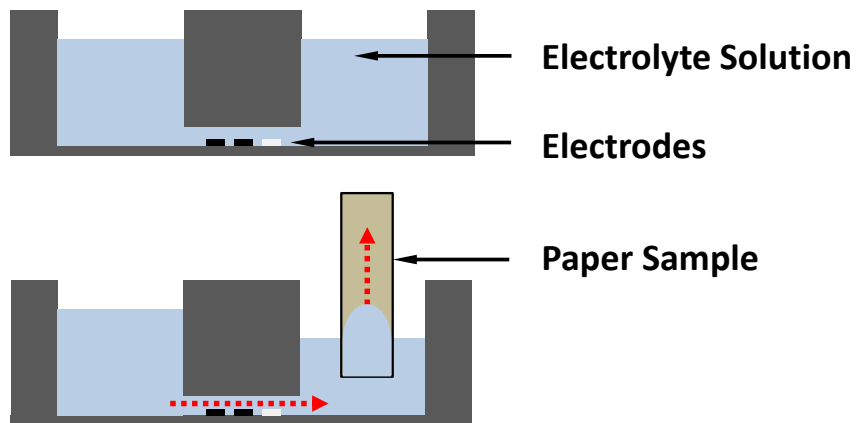


Figure 24. Schematic illustrations of flow operation, induced by a paper sample in the device system; paper sample is loaded to the electrolyte filled device's reservoir then fluid flow is induced channel inside, then electrochemical signal reading will be follow according to the flow rate.

3.3 Results and Discussion

3.3.1 Flow Measurement

Flow mechanism

As shown in **Figure 25A**, a plot of current versus time is measured electrochemically from the moment of dipping the paper into the device. The red line means current over time, which is gained by electrochemical detection. The black line means flow rate over time, which is calculated via theoretical equation from measured current. Generally, these two curves have the same mechanisms appearances; after the introduction of paper to the electrolyte solution filled device, there is a wet-out state rely on surface tension effect as formalized by Washburn equation. After then, capillary force based fully-wetted out state flow is followed. Finally, after absorption as much as the paper does, saturation is occurred and it is revealed by decreased current. To characterize the fully-wetted flow state from the whole flowing mechanisms, derivatives of the flow rate is analyzed (**Figure 25B**). From a local minimum time ($x=t_1$ to t_2), where $y=0$, fully-wetted flow is defined.

Calibration

To evaluate the performance of device, a syringe pump is connected to the outlet reservoir of the device and it is utilized to induce a range of flow rate: 5, 10, 20, and 30 $\mu\text{L}/\text{sec}$. Each flow rate continues for 15 seconds, respectively. During the gradually increased flow generation, electrochemical measurement is taken constantly (**Figure 26A**). In the **Figure 26B**, the red dashed line represents a linear fitting curve with the average value of 4 times of experimentally measured flow rate: $y = 15.990x + 2.5117$ ($R^2 = 0.99883$). The black line is a theoretically calculated curve. Through the comparison of the calibration data and theoretical basis, the suitability of the proposed device is confirmed.

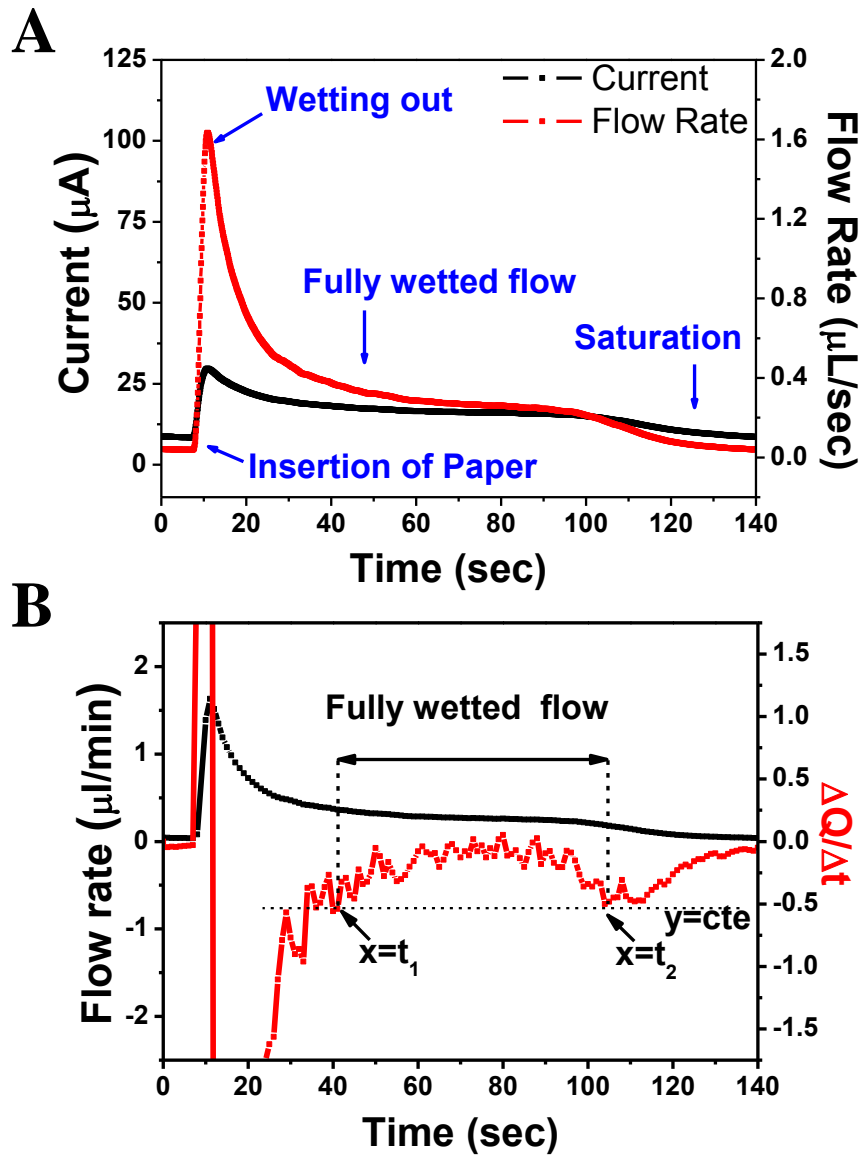


Figure 25. Electrochemically measured fluid flow induced by porous materials. (A) Flow mechanisms derived by porous material from insertion of paper to saturation generating wetting out state flow and fully wetted state flow in-between. (B) Characterization method of the fully-wetted flow state by using derivative flow rate.

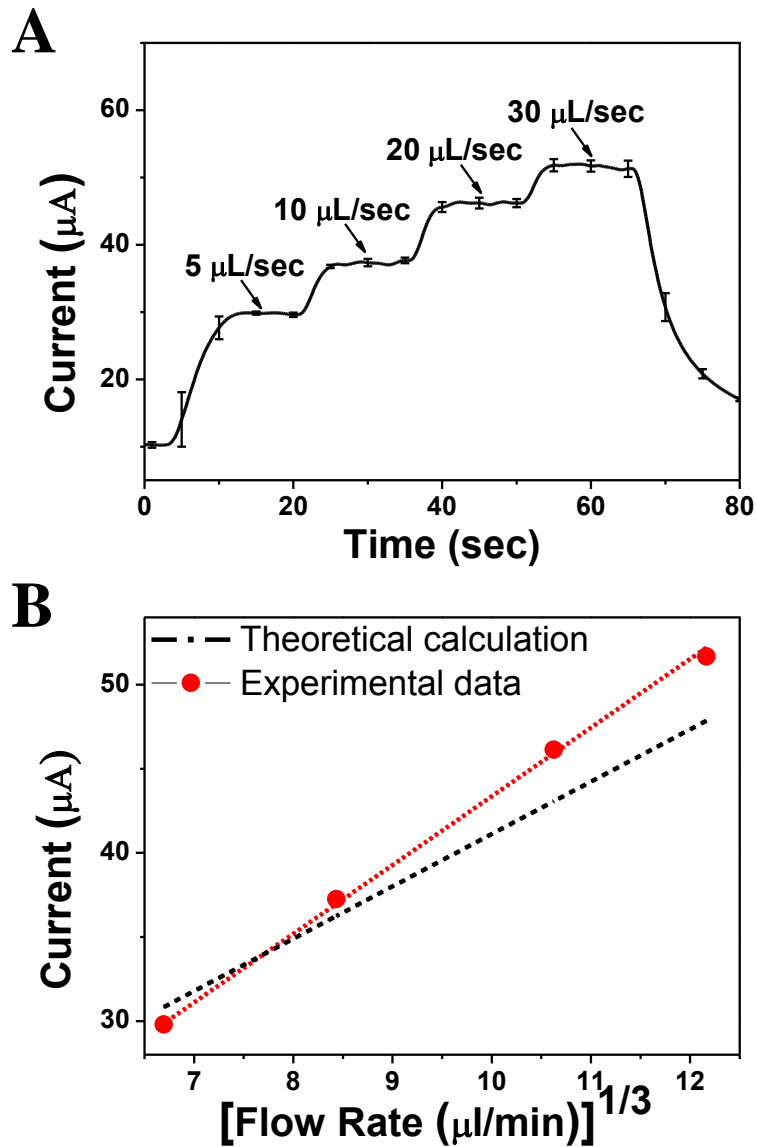


Figure 26. Calibration curves of electrochemically measured results using the proposed device. (A) Current measurement of a range of flow rate induced by an increasing programmed syringe pump. (B) Calibration curves gained by experimental measurement and theoretical calculation.

3.3.2 Characterization of Flow Rate

There are three different characteristic analyses of porous material using the device: different geometric effect with same material strips, flow duration time analysis by different size of absorbance pads, and different products test with same geometric structure (**Figure 27 to 29**).

Geometric effect

The different geometric paper is distinguished: 3, 6, and 12mm width (**Figure 27A**). Even though all of tested strips have the same material compositions and the same length; the particular width makes a significant change to the porous material's flow rate. As expected from the Darcy's law, the strip with 3mm width has the slowest flow rate than others in this experiment, while the strip with 12mm width has the fastest flow rate among the three samples. The width of the paper has proportional relation with the flow rate. Furthermore, volume absorbed by each paper has a linear enhancement as width of papers become wider (**Figure 27B**). To calculate this, flow rate is accepted by fully-wetted state flow as shown in **Figure 25B**. A black dotted line is a linear fitting curve of the absorbed volume to the strip, which is displaced by integration of experimental results and the red dotted line shows the absorbed volume to the strip, which is the measured mass by a scale. As results, these two graphs are relatively overlapped, which gives evidence of suitability of the device. The flow rate magnitudes proportional relation between paper width and flow rate (**Figure 27C**).

Duration time

In **figure 28A**, paper fluidics is demonstrated with a distinguishing duration time depending on the size of absorbance pads. All strips are cut in the dimension of 3mm×5cm. The square shaped additionally patched pads are connected to the end point of the strips: 1×1, 2×2, and 3×3 pads. Through this, flowing duration time of fully wetted flow stays longer and the total absorbed volume become bigger depending on the pad's size (**Figure 28B**). Absorption capacity of the different papers is dramatically enhanced from approximately 20 seconds for no pad to 40, 105, and 208 seconds for, respectively. However, the averaged fully wetted flow rates of each pad are maintained as a constant value, which is determined parameter by the paper material or size (**Figure 28C**).

Product analysis

Maintaining similar dimensions (3mm×5cm), different types of papers have various hydrodynamic capabilities due to diverse reasons such as porosity, density or surface coating. In **Figure 29A**, two kinds of absorbance pads (Pall 111 and Pall 133), filter paper (whatman), and nitrocellulose membrane have evaluated in terms of flow rate. It is clear that the different product of paper generates a unique flow behavior. Typically, absorbance pad has less dense property than filter paper or

nitrocellulose membrane, resulting in faster flow rate than other types of paper. Statistical analysis of the fully wetted phase shows the NC or whatman paper strips in extending the flow while minimizing the flow rate magnitude (**Figure 29B**).

Flow modification

Flow modification techniques are tested using water soluble DEX valve and oxygen plasma pump. It is evaluated in the comparison with normal nitrocellulose membrane, and all of strips geometries are same as 6mm×6cm size by observing color dyed water profiles visually. The oxygen plasma treated strip takes around 3 minutes to saturate, while DEX valve treated strip takes around 10 minutes to saturate because, fluid flow is permanently blocked at position of DEX band. The quantitative analysis of the flow modifiers are obtained by visual monitoring of dye decorated aqueous solution transport (**Figure 30**). The quantitative analysis of the fluid flow modifiers using the device with chronoamperometric measurement matched the results obtained by visual monitoring of dye decorated aqueous solution transport. The flow rate signature for plasma treated NC paper strips showed high magnitude than non-treated paper strips (**Figure 31A**). Also, the performance of water-soluble valves using 8, 12 and 20%_{w/v} DEX shows the significant reduction of the flow rate (**Figure 31B**).

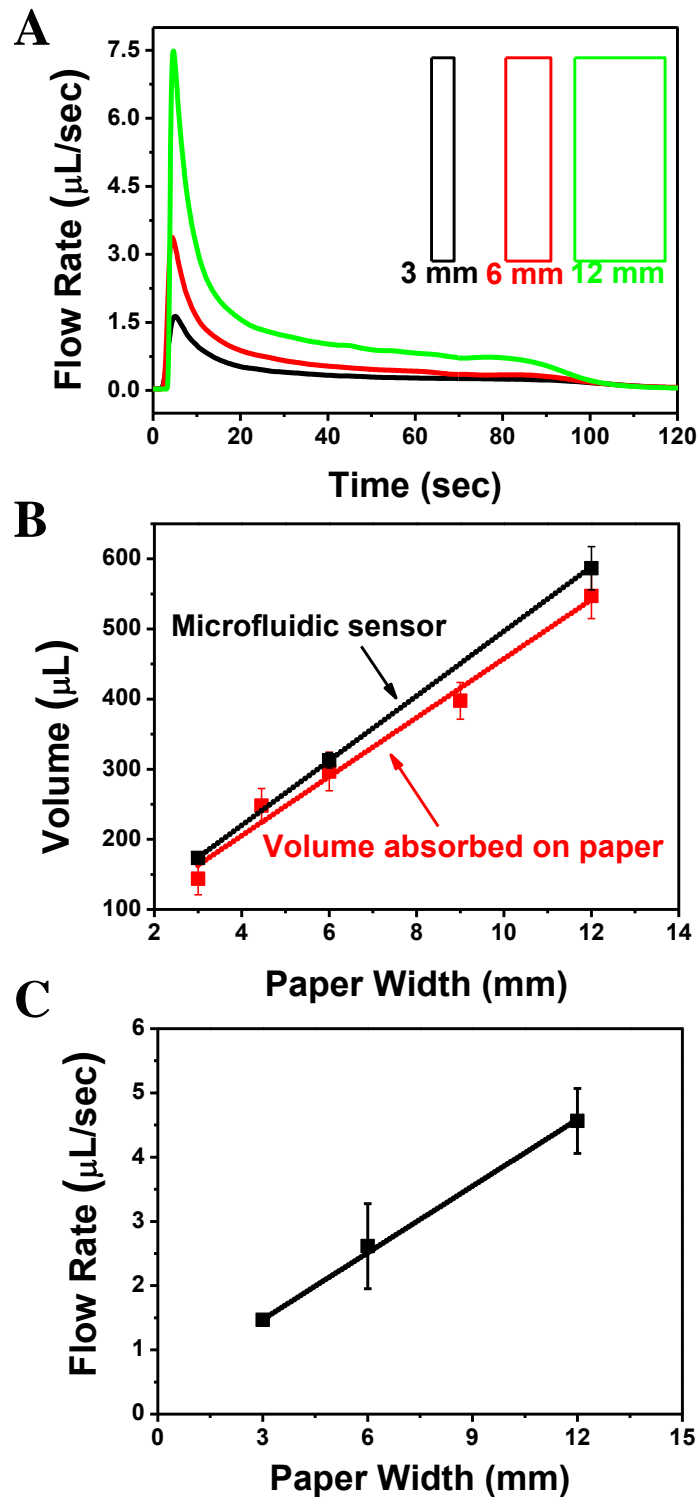


Figure 27. Analysis of geometric effect in flow rate. (A) Flow rates from different width's paper: 3, 6 and 12mm. (B) Relationship between paper width and volume absorbed by the paper. Two calibration curves are generated by microfluidic sensor based measurement and direct measurement using mass balance of solution absorbed. (C) Linear proportional relation between paper width and the flow rate.

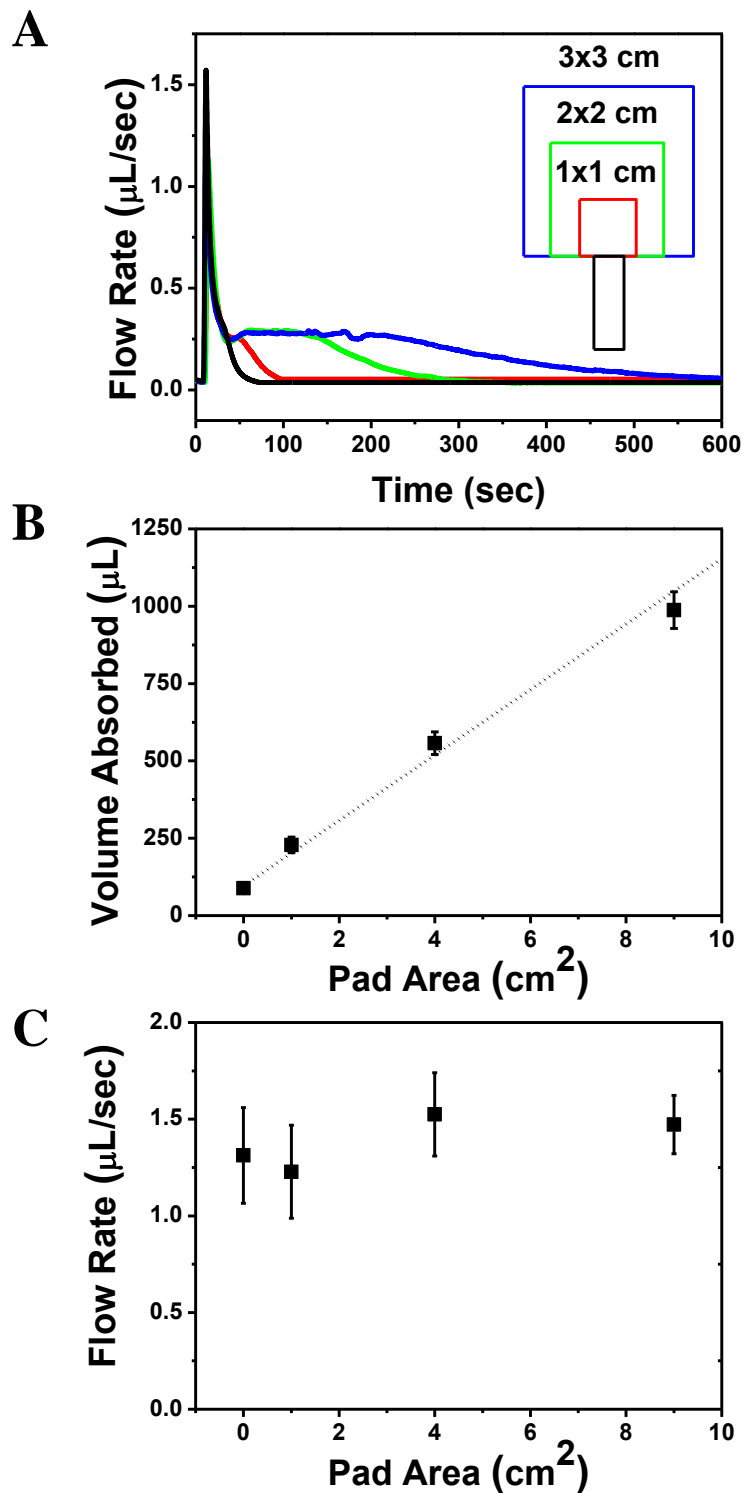


Figure 28. Analysis of additional absorbing pad's effect. (A) Flow rates from different surface area's pads: 0×0 , 1×1 , 2×2 , and 3×3 cm^2 . (B) Linear proportional relation between absorbing pad's surface area and the volume absorbed. (C) Steady flow rates from different surface area's pads. For each area, three sets of experiments are tried.

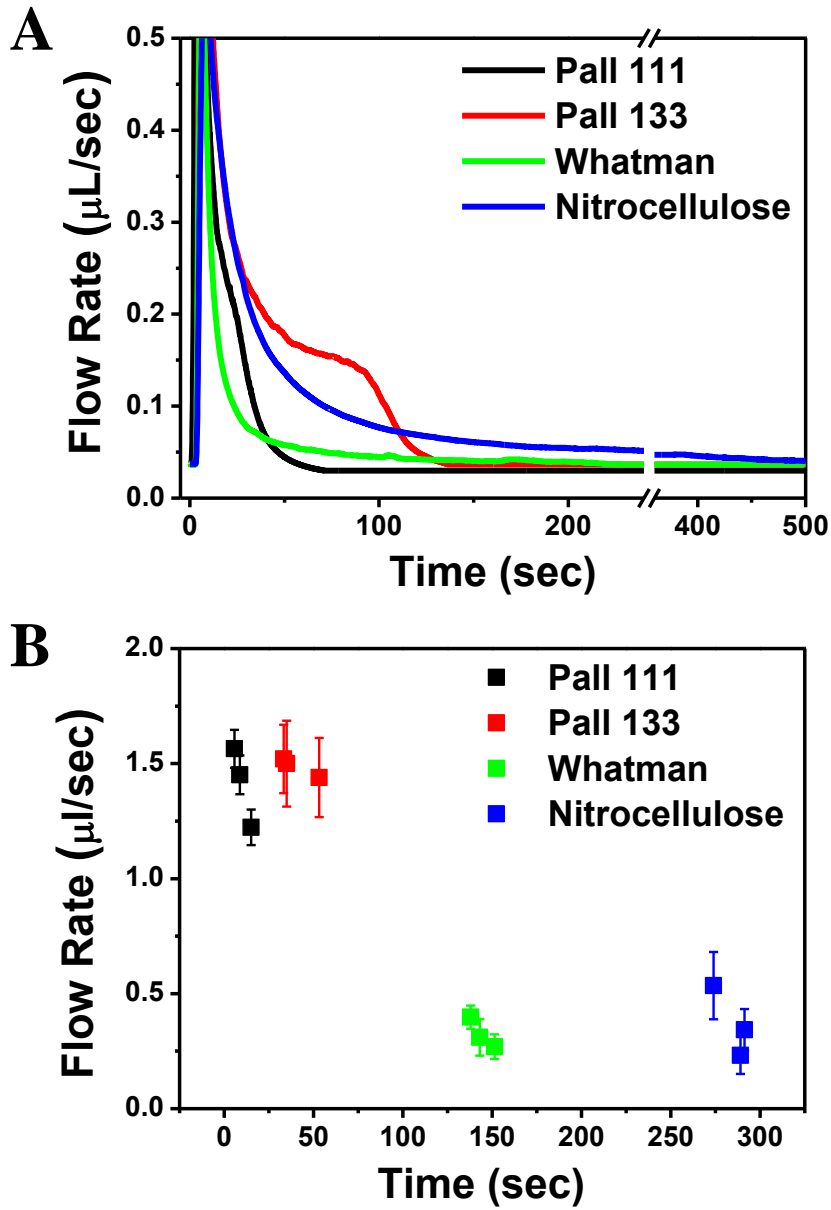


Figure 29. Analysis of flow mechanisms from different paper products. (A) Different material based paper products show diverse flow rate profile. (B) Average analysis of flow duration time to flow rate from diverse paper samples.

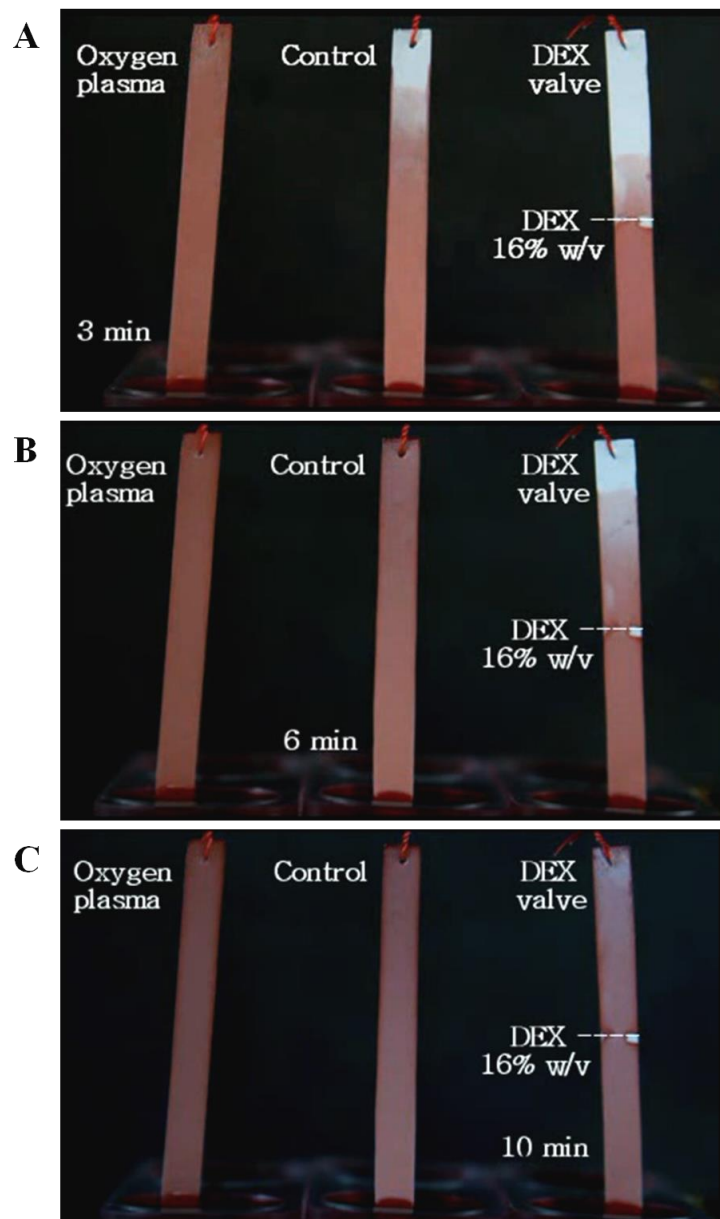


Figure 30. Characterization of fluid modification by applying oxygen plasma treated, 16% w/v dextran coated, and normal nitrocellulose membrane. Oxygen plasma treated paper shows the fastest flow duration time until saturation, while DEX valve coated paper shows the longest duration time until saturation.

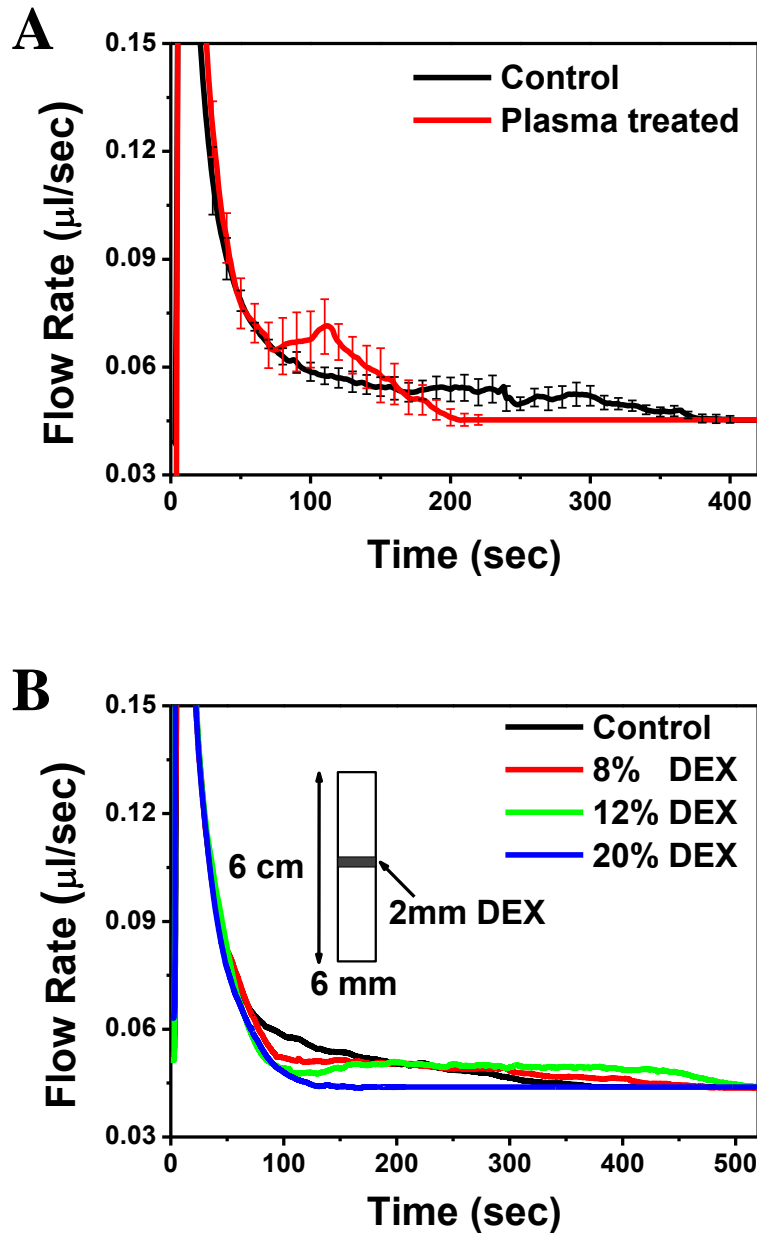


Figure 31. Characterization of fluid modifiers by using electrochemical measurement system. (A) The fully wetted flow rate magnitude for oxygen plasma treated paper strips and non-treated paper strips (n=7). (B) The dependent delay time of paper strip wicking using DEX valve of 8, 12, and 20%_{w/v}, respectively.

3.4 Conclusion

In this study, a novel non-invasive flow monitoring system for the fluid flow through the strip sensors and porous materials is presented. Based on the electrochemical velocimetry method, which evaluate the capillary mediated flow rate of a liquid through a porous sample, it is able to measure wetting behavior with accurate and straightforward technique. It does not require the modification or alteration of the sample and allows any type of porous media to be tested. The sensitivity of the flow measurement technique is confirmed by the characterization of different geometry or composition derived flow. Also, flow control by applying different type of modifiers suggests the potential of diverse applications.

Monitoring hydrodynamic behaviors derived by paper based microfluidic devices allows the evaluation of wetting capabilities of the system. Via this study, it can be used in quality control test for the flow monitoring and/or the quality control of other porous materials. Overall, this technique is successfully recorded capillary-drive flow generated by paper based system.

4 Concluding Remarks

Overall, electrochemical measurement in microfluidic system is developed as an alternative for the optical detection which requires optically transparent materials. As an electrochemical detection is not dependent on the optical properties, it is possible that the device can be made of any materials, eliminating the need to make devices out of costly plastics, such as COC or PMMA. Through this, not only a microfluidic disc with embedded miniaturized electrochemical sensors, but also flow rate monitoring technique is developed in this study. Cost effective, high sensitive and fully automated lab-on-a-disc immunosensor is successfully developed and it has comparable sensitivity with gold electrode via flow enhanced signal. Also, simple, noninvasive and straightforward fluid flow monitoring technique is introduced.

References

1. www.photron.com.
2. <http://www.mf20.org/practical-guide-fluid-flow-porous-media>.
3. www.p-wholesale.com
4. www.samsungmedison.co.kr.
5. Linder, V.; Sia, S. K.; Whitesides, G. M., Reagent-loaded cartridges for valveless and automated fluid delivery in microfluidic devices. *Analytical chemistry* **2005**, *77* (1), 64-71.
6. Noroozi, Z.; Kido, H.; Madou, M. J., Electrolysis-Induced Pneumatic Pressure for Control of Liquids in a Centrifugal System. *Journal of The Electrochemical Society* **2011**, *158* (11), P130-P135.
7. Park, J.-M.; Cho, Y.-K.; Lee, B.-S.; Lee, J.-G.; Ko, C., Multifunctional microvalves control by optical illumination on nanoheaters and its application in centrifugal microfluidic devices. *Lab on a Chip* **2007**, *7* (5), 557-564.
8. Ducrée, J.; Haeberle, S.; Lutz, S.; Pausch, S.; Von Stetten, F.; Zengerle, R., The centrifugal microfluidic bio-disk platform. *Journal of Micromechanics and Microengineering* **2007**, *17* (7), S103.
9. Martinez, A. W.; Phillips, S. T.; Whitesides, G. M., Three-dimensional microfluidic devices fabricated in layered paper and tape. *Proceedings of the National Academy of Sciences* **2008**, *105* (50), 19606-19611.
10. www.alere.com
11. Civit, L.; Fragoso, A.; O'Sullivan, C., Electrochemical biosensor for the multiplexed detection of human papillomavirus genes. *Biosensors and Bioelectronics* **2010**, *26* (4), 1684-1687.
12. www.medicalexpo.com.
13. Duffy, D. C.; Gillis, H. L.; Lin, J.; Sheppard, N. F.; Kellogg, G. J., Microfabricated centrifugal microfluidic systems: characterization and multiple enzymatic assays. *Analytical Chemistry* **1999**, *71* (20), 4669-4678.
14. Madou, M.; Zoval, J.; Jia, G.; Kido, H.; Kim, J.; Kim, N., Lab on a CD. *Annu. Rev. Biomed. Eng.* **2006**, *8*, 601-628.
15. Fu, E.; Ramsey, S. A.; Kauffman, P.; Lutz, B.; Yager, P., Transport in two-dimensional paper networks. *Microfluid Nanofluidics* **2011**, *10* (1), 29-35.
16. <http://mediconweb.com/health-wellness/home-pregnancy-test-indications-procedure-and-results/#.UykRATOKC70>.
17. Mark, D.; Metz, T.; Haeberle, S.; Lutz, S.; Ducrée, J.; Zengerle, R.; von Stetten, F.,

- Centrifugo-pneumatic valve for metering of highly wetting liquids on centrifugal microfluidic platforms. *Lab on a Chip* **2009**, *9* (24), 3599-3603.
18. Lee, B. S.; Lee, Y. U.; Kim, H.-S.; Kim, T.-H.; Park, J.; Lee, J.-G.; Kim, J.; Kim, H.; Lee, W. G.; Cho, Y.-K., Fully integrated lab-on-a-disc for simultaneous analysis of biochemistry and immunoassay from whole blood. *Lab on a Chip* **2011**, *11* (1), 70-78.
 19. www.quidel.com.
 20. Lai, S.; Wang, S.; Luo, J.; Lee, L. J.; Yang, S.-T.; Madou, M. J., Design of a Compact Disk-like Microfluidic Platform for Enzyme-Linked Immunosorbent Assay. *Analytical Chemistry* **2004**, *76* (7), 1832-1837.
 21. Weaver, A. A.; Reiser, H.; Barstis, T.; Benvenuti, M.; Ghosh, D.; Hunckler, M.; Joy, B.; Koenig, L.; Raddell, K.; Lieberman, M., Paper Analytical Devices for Fast Field Screening of Beta Lactam Antibiotics and Antituberculosis Pharmaceuticals. *Analytical Chemistry* **2013**, *85* (13), 6453-6460.
 22. Abi-Samra, K.; Kim, T. H.; Park, D. K.; Kim, N.; Kim, J.; Kim, H.; Cho, Y. K.; Madou, M., Electrochemical velocimetry on centrifugal microfluidic platforms. *Lab Chip* **2013**, *13* (16), 3253-60.
 23. Liang, W.; Li, Y.; Zhang, B.; Zhang, Z.; Chen, A.; Qi, D.; Yi, W.; Hu, C., A novel microfluidic immunoassay system based on electrochemical immunosensors: An application for the detection of NT-proBNP in whole blood. *Biosensors and Bioelectronics* **2012**, *31* (1), 480-485.
 24. www.abc-residue.com.
 25. Lee, B. S.; Lee, J.-N.; Park, J.-M.; Lee, J.-G.; Kim, S.; Cho, Y.-K.; Ko, C., A fully automated immunoassay from whole blood on a disc. *Lab on a Chip* **2009**, *9* (11), 1548-1555.
 26. Li, T.; Fan, Y.; Cheng, Y.; Yang, J., An electrochemical Lab-on-a-CD system for parallel whole blood analysis. *Lab Chip* **2013**.
 27. Park, J.; Sunkara, V.; Kim, T.-H.; Hwang, H.; Cho, Y.-K., Lab-on-a-Disc for Fully Integrated Multiplex Immunoassays. *Analytical Chemistry* **2012**, *84* (5), 2133-2140.
 28. Fu, E.; Lutz, B.; Kauffman, P.; Yager, P., Controlled reagent transport in disposable 2D paper networks. *Lab Chip* **2010**, *10* (7), 918-20.
 29. Fraiwan, A.; Mukherjee, S.; Sundermier, S.; Lee, H. S.; Choi, S., A paper-based microbial fuel cell: instant battery for disposable diagnostic devices. *Biosensors & bioelectronics* **2013**, *49*, 410-4.
 30. Kim, T. H.; Abi-Samra, K.; Sunkara, V.; Park, D. K.; Amasia, M.; Kim, N.; Kim, J.; Kim, H.; Madou, M.; Cho, Y. K., Flow-enhanced electrochemical immunosensors on centrifugal microfluidic platforms. *Lab Chip* **2013**, *13* (18), 3747-54.

31. Honda, N.; Lindberg, U.; Andersson, P.; Hoffmann, S.; Takei, H., Simultaneous multiple immunoassays in a compact disc-shaped microfluidic device based on centrifugal force. *Clinical chemistry* **2005**, *51* (10), 1955-1961.
32. Gravesen, P.; Branebjerg, J.; Jensen, O. S., Microfluidics-a review. *Journal of Micromechanics and Microengineering* **1993**, *3* (4), 168.
33. Whitesides, G. M., The origins and the future of microfluidics. *Nature* **2006**, *442* (7101), 368-73.
34. Liu, H.; Crooks, R. M., Paper-based electrochemical sensing platform with integral battery and electrochromic read-out. *Analytical chemistry* **2012**, *84* (5), 2528-2532.
35. Morais, S.; Carrascosa, J.; Mira, D.; Puchades, R.; Maquieira, Á., Microimmunoanalysis on standard compact discs to determine low abundant compounds. *Analytical chemistry* **2007**, *79* (20), 7628-7635.
36. Chin, C. D.; Linder, V.; Sia, S. K., Lab-on-a-chip devices for global health: past studies and future opportunities. *Lab on a Chip* **2007**, *7* (1), 41-57.
37. Myers, F. B.; Lee, L. P., Innovations in optical microfluidic technologies for point-of-care diagnostics. *Lab Chip* **2008**, *8* (12), 2015-31.
38. Sia, S. K.; Kricka, L. J., Microfluidics and point-of-care testing. *Lab Chip* **2008**, *8* (12), 1982-3.
39. Yager, P.; Edwards, T.; Fu, E.; Helton, K.; Nelson, K.; Tam, M. R.; Weigl, B. H., Microfluidic diagnostic technologies for global public health. *Nature* **2006**, *442* (7101), 412-8.
40. Apilux, A.; Ukita, Y.; Chikae, M.; Chailapakul, O.; Takamura, Y., Development of automated paper-based devices for sequential multistep sandwich enzyme-linked immunosorbent assays using inkjet printing. *Lab Chip* **2013**, *13* (1), 126-35.
41. Gorkin, R.; Park, J.; Siegrist, J.; Amasia, M.; Lee, B. S.; Park, J. M.; Kim, J.; Kim, H.; Madou, M.; Cho, Y. K., Centrifugal microfluidics for biomedical applications. *Lab Chip* **2010**, *10* (14), 1758-73.
42. Chin, C. D.; Laksanasopin, T.; Cheung, Y. K.; Steinmiller, D.; Linder, V.; Parsa, H.; Wang, J.; Moore, H.; Rouse, R.; Umvilighozo, G.; Karita, E.; Mwambarangwe, L.; Braunstein, S. L.; van de Wijgert, J.; Sahabo, R.; Justman, J. E.; El-Sadr, W.; Sia, S. K., Microfluidics-based diagnostics of infectious diseases in the developing world. *Nature medicine* **2011**, *17* (8), 1015-9.
43. Haber, C., Microfluidics in commercial applications; an industry perspective. *Lab Chip* **2006**, *6* (9), 1118-21.
44. Li, X.; Ballerini, D. R.; Shen, W., A perspective on paper-based microfluidics: Current status

- and future trends. *Biomicrofluidics* **2012**, *6*, 011301.
45. Hessel, V.; Löwe, H.; Schönfeld, F., Micromixers—a review on passive and active mixing principles. *Chemical Engineering Science* **2005**, *60* (8), 2479-2501.
 46. Mansur, E. A.; YE, M.; WANG, Y.; DAI, Y., A state-of-the-art review of mixing in microfluidic mixers. *Chinese Journal of Chemical Engineering* **2008**, *16* (4), 503-516.
 47. Grumann, M.; Geipel, A.; Riegger, L.; Zengerle, R.; Ducree, J., Batch-mode mixing on centrifugal microfluidic platforms. *Lab Chip* **2005**, *5* (5), 560-5.
 48. Fu, E.; Liang, T.; Spicar-Mihalic, P.; Houghtaling, J.; Ramachandran, S.; Yager, P., Two-dimensional paper network format that enables simple multistep assays for use in low-resource settings in the context of malaria antigen detection. *Anal Chem* **2012**, *84* (10), 4574-9.
 49. Klasner, S. A.; Price, A. K.; Hoeman, K. W.; Wilson, R. S.; Bell, K. J.; Culbertson, C. T., Paper-based microfluidic devices for analysis of clinically relevant analytes present in urine and saliva. *Analytical and bioanalytical chemistry* **2010**, *397* (5), 1821-1829.
 50. Andres W. Martinez, S. T. P., and George M. Whitesides, Diagnostics for the Developing World: Microfluidic Paper-based analytical Devices. *Analytical chemistry* **2010**, *82*, 3-10.
 51. Yetisen, A. K.; Akram, M. S.; Lowe, C. R., Paper-based microfluidic point-of-care diagnostic devices. *Lab Chip* **2013**, *13* (12), 2210-51.
 52. Osborn, J. L.; Lutz, B.; Fu, E.; Kauffman, P.; Stevens, D. Y.; Yager, P., Microfluidics without pumps: reinventing the T-sensor and H-filter in paper networks. *Lab Chip* **2010**, *10* (20), 2659-65.
 53. Szekely, J.; Neumann, A.; Chuang, Y., The rate of capillary penetration and the applicability of the Washburn equation. *Journal of Colloid and Interface Science* **1971**, *35* (2), 273-278.
 54. Milipore, Rapid Lateral Flow Test Strips.
 55. Blake, C.; Gould, B. J., Use of enzymes in immunoassay techniques. A review. *Analyst* **1984**, *109* (5), 533-547.
 56. Chan, D. W., *General principle of immunoassay*. 1987; p 1-23.
 57. Pauling, L., *The specificity of serological reactions*. Harvard University Press: 1945.
 58. Darwish, I. A., Immunoassay Methods and their Applications in pharmaceutical Analysis: Basic Methodology and Recent Advances. *International journal of biomedical science* **2006**, *2* (3), 217-235.
 59. Gervais, L.; de Rooij, N.; Delamarche, E., Microfluidic chips for point-of-care immunodiagnosics. *Advanced materials* **2011**, *23* (24), H151-76.
 60. Sato, K.; Tokeshi, M.; Odake, T.; Kimura, H.; Ooi, T.; Nakao, M.; Kitamori, T., Integration of an immunosorbent assay system: analysis of secretory human immunoglobulin A on

- polystyrene beads in a microchip. *Analytical Chemistry* **2000**, 72 (6), 1144-1147.
61. Heyries, K. A.; Mandon, C. A.; Ceriotti, L.; Ponti, J.; Colpo, P.; Blum, L. J.; Marquette, C. A., "Macromolecules to PDMS transfer" as a general route for PDMS biochips. *Biosensors and Bioelectronics* **2009**, 24 (5), 1146-1152.
 62. Darain, F.; Yager, P.; Gan, K. L.; Tjin, S. C., On-chip detection of myoglobin based on fluorescence. *Biosensors and Bioelectronics* **2009**, 24 (6), 1744-1750.
 63. Lin, C.-C.; Wang, J.-H.; Wu, H.-W.; Lee, G.-B., Microfluidic Immunoassays. *Journal of the Association for Laboratory Automation* **2010**, 15 (3), 253-274.
 64. Kim, D.; Herr, A. E., Protein immobilization techniques for microfluidic assays. *Biomicrofluidics* **2013**, 7 (4), 041501.
 65. Herr, A. E.; Hatch, A. V.; Throckmorton, D. J.; Tran, H. M.; Brennan, J. S.; Giannobile, W. V.; Singh, A. K., Microfluidic immunoassays as rapid saliva-based clinical diagnostics. *Proceedings of the National Academy of Sciences* **2007**, 104 (13), 5268-5273.
 66. Gervais, L.; Delamarche, E., Toward one-step point-of-care immunodiagnostics using capillary-driven microfluidics and PDMS substrates. *Lab on a Chip* **2009**, 9 (23), 3330-3337.
 67. Kuswandi, B.; Huskens, J.; Verboom, W., Optical sensing systems for microfluidic devices: a review. *Analytica chimica acta* **2007**, 601 (2), 141-155.
 68. *Lateral_Flow_Immunoassay*. Springer: 2009.
 69. Han, K. N.; Li, C. A.; Seong, G. H., Microfluidic chips for immunoassays. *Annual review of analytical chemistry* **2013**, 6, 119-41.
 70. Bard, A. J.; Faulkner, L. R., *Electrochemical methods: fundamentals and applications*. Wiley New York: 1980; Vol. 2.
 71. Compton, R. G.; Banks, C. E., *Understanding voltammetry*. World Scientific: 2007.
 72. Fanjul-Bolado, P.; González-García, M. B.; Costa-García, A., Amperometric detection in TMB/HRP-based assays. *Analytical and Bioanalytical chemistry* **2005**, 382 (2), 297-302.
 73. Müller, R.; Clegg, D. L., Automatic paper chromatography. *Analytical Chemistry* **1949**, 21 (9), 1123-1125.
 74. Müller, R. H.; Clegg, D. L., Automatic Paper Chromatography. *Annals of the New York Academy of Sciences* **1951**, 53 (5), 1108-1118.
 75. Rebe Raz, S.; Haasnoot, W., Multiplex bioanalytical methods for food and environmental monitoring. *TrAC Trends in Analytical Chemistry* **2011**, 30 (9), 1526-1537.
 76. Barr, M. C.; Rowehl, J. A.; Lunt, R. R.; Xu, J.; Wang, A.; Boyce, C. M.; Im, S. G.; Bulović, V.; Gleason, K. K., Direct monolithic integration of organic photovoltaic circuits on unmodified paper. *Advanced materials* **2011**, 23 (31), 3500-3505.
 77. Lokendra Pal, M. K. J., and Paul D. Fleming, A simple method for calculation of the

permeability coefficient of porous media. *PEER-REVIEWED PAPER PHYSICS 5.*

Acknowledgements

First of all, I would like to express my deepest appreciation to my advisor Professor Yoon-Kyoung Cho for her great guidance, enthusiasm and complete support for my master study and research. I have been amazingly fortunate to have an advisor who gave me the belief confidence to explore on my own. Her patience and support made me improve in many ways. Without her guidance and persistent help, this dissertation would not have been possible. Also, I wish to express my sincere thanks to my committee members, Professor Chang-Young Lee and Professor Marc J. Madou for their encouragement, insightful comments and constructive questions.

In addition, I appreciate Dr. Kameel, Dr. Cedric, and Dr. Tae-Hyeong for their grateful advices and ideas working with electrochemical detection projects. I specially thank Juhee Park and Ada Lee, for their encouragement and comments over the period of my master course. Also, I am grateful to all of FRUITS lab members, who helped me a lot to prepare my thesis and defense presentation.

Many friends have helped me stay here through this difficult time. Their support, encouraging, comments, and a lot of prayer helped me overcome difficulties. I deeply appreciate them.

Most importantly, none of this would have been possible without the love and patience of my family. They have provided the endless support through my entire life. Last but not least, I must acknowledge my love, SW.

Curriculum Vitae

Ja-Ryoung Han

M.S.

Department of Chemical Engineering

Ulsan National Institute of Science and Technology (UNIST), Ulsan City, Republic of Korea

Mobile : +82-10-3126-1231

E-mail : folori@hanmail.net

EDUCATION

M.S, Chemical Engineering, 2014, UNIST, Ulsan, Republic of Korea

B.A, Chemical Engineering, 2012, Kyungpook National University, Daegu, Republic of Korea

RESEARCH INTERESTS

- Electrochemistry, screen-printed carbon electrodes
- Microfluidics: lab-on-a-disc, paper based microfluidics
- Immunoassay, fluid dynamics

RESEARCH PUBLICATIONS

1. C. Bathany†; **J.-R. Han**†; K. Abi-Samra; S.Takayama and Y.-K. Cho, “Noninvasive flow measurement in porous material by an electrochemical sensor system”, in preparation, 2014, † equally contributed.
2. W. S Lee; V. Sunkara; **J.-R. Han**; Y.-S Park; Y.-K. Cho, “Electrospun TiO₂ Nanofiber Integrated Lab-on-a-Disc for Ultrasensitive Protein Detection from Whole Blood”, *Advanced Health Materials*, submitted, 2014.
3. [PATENT] Y.-K. Cho, K. Abi-Samra; **J.-R. Han**, “Method to measure flow in porous materials”, UTP13126KR-00, in pending, 2013.

CONFERENCES

1. Ja-Ryoung Han, Kameel Abi-Samra, and Cédric Bathany and Yoon-Kyoung Cho. “Real-time flow measurement in paper-based microfluidics”, *microTAS 2013 conference*, 27-31 October, Freiburg, Germany
2. Yang-Seok Park, Won Seok Lee, Vijaya Sunkara, Ja-Ryoung Han and Yoon-Kyoung Cho, “Nanofiber-based Ultrasensitive Immunoassay Integrated on a Centrifugal Microfluidic Device”, *Gordon Research Conference, Physics & Chemistry of Microfluidics*, June 9 - 14,

2013, Lucca, Italy

3. Kameel Abi-Samra, Ja-Ryoung Han and Yoon-Kyoung Cho, “Electrochemical Velocimetry in Paper-Based microfluidics”, *Advances in Microfluidics & Nanofluidics 2013*, Notre Dame, IN, USA, May 24-26, 2013.
-

HONORS

- 2012.08 – 2014.02 RA/TA scholarship, UNIST
 - 2012.03 – 2012.06 National Scholarship, KNU
 - 2012.03 - 2012.06 Vision Scholarship, KNU
 - 2011.03 – 2011.06 Scholarship for Academic Excellence, KNU
 - 2010.09 – 2010.12 Vision Scholarship, KNU
 - 2010.09 – 2010.12 Curriculum empowerment scholarship, KNU
-

AWARDS

- 2011.02.10 Convergence creative design contest, Hong-Ik university president award, Convergence education center
 - 2010.10.22 Creative design contest, silver prize, Korean institute of Chemical engineering
-